Quasi-Free Scattering and Nuclear Structure*

GERHARD JACOB, TH. A. J. MARIS
Instituto de Física and Faculdade de Filosofia, Universidade do Rio Grande do Sul, Pôrto Alegre, Brasil

Quasi-free processes in nuclei are reviewed both from a theoretical and an experimental point of view. The discussion is limited to nuclei with mass number ≥ 4 and to incident energies larger than 100 MeV for quasi-free proton–proton and 300 MeV for electron–proton scattering. The reactions are discussed qualitatively, and their relevance for the investigation of nuclear shells, in particular of the strongly bound ones, is shown. The cross section for quasi-free scattering is then derived in the distorted wave impulse approximation, and some special cases are considered. Through a few examples the main features of the experimental results are presented and compared with calculated ones. Measurements on several $1p$, $2s$–$1d$, and $2p$–$1f$ shell nuclei are discussed.

CONTENTS

I. INTRODUCTION

In the last fifteen years the shell model[1] has been successful in the explanation of numerous properties of the nucleus. With respect to the domain of validity of the model, it should, however, be remarked that although the existence of strongly bound shells in nuclei seems to be implied, nearly all experiments performed until recently have been restricted to investigations of the least bound and of the unoccupied shells. To test the shell model predictions for the more strongly bound shells, these have to be broken up, and consequently a relatively high energy is needed; for decay experiments and scattering at low energies the core of the nucleus somewhat resembles an elementary particle of which only over-all properties are relevant and can be determined.

As the energy differences between neighboring shells vary from about 25 MeV for light nuclei to probably less than 10 MeV for heavy ones, one could expect that experiments with nucleons of a medium energy, larger than these differences but substantially smaller than 100 MeV might be suitable for investigations of inner shells. This is not the case because the mean free path of nucleons for those energies is relatively small and surface reactions occur almost exclusively. The nuclear surface, however, consists predominantly of upper shell particles because of the sloping edges of the shell model potential and, also, due to the dependence of the exponential tail of a single-particle wave function on its separation energy. (We use the term separation energy in a generalized sense, defining it as the energy necessary to lift any bound nucleon, not only the least bound one, to zero energy). When photons are used as projectiles, only the lower energy limitation exists because gammas have a long mean free path in nuclear matter. Actually, the giant dipole gamma resonance was the first excitation for which it became clear that particles from a closed inner shell (namely, the next to the upper one) can be involved.[2] However, medium energy gammas have a wavelength which is considerably larger than the average internucleon distance and, therefore, excite almost exclusively collective modes.[3] In fact, another reason for the use of a high bombarding energy is that a high momentum transfer results in a localized interaction which emphasizes single-particle properties.

Experiments which are particularly suited to investigate the inner nuclear shell structure are the quasi-free (also called quasi-elastic) scattering experiments. Qualitatively speaking, by quasi-free scattering a process is meant in which a high energy (100–1000 MeV) particle knocks a nucleon out of a nucleus and no further violent interaction occurs between the nucleus and the incident or the two outgoing particles. Because the mean free path of high energy nucleons in nuclear matter is of the same order of magnitude as the nuclear radius such events are expected to be reasonably probable.[4]

The first experiments demonstrating the existence of such processes were performed at Berkeley[5] in 1952 by the bombardment of light nuclei with 340-MeV protons and the observation of coincident proton pairs emerging from the target with a strong angular correlation. Semiquantitatively,[4,6] these events can be described

* This review is based on a paper submitted by one of us (G.J.) to the Faculdade de Filosofia, Universidade do Rio Grande do Sul, in partial fulfillment of the requirements for the Chair of Theoretical Physics.

[1] M. G. Mayer and J. H. D. Jensen, *Elementary Theory of Nuclear Shell Structure* (John Wiley & Sons, Inc., New York, 1955).

[2] D. H. Wilkinson, Physica **22**, 1039 (1956).

[3] G. E. Brown and M. Bolsterli, Phys. Rev. Letters **3**, 472 (1959).

[4] R. Serber, Phys. Rev. **72**, 1114 (1947); M. L. Goldberger, Phys. Rev. **74**, 1269 (1948).

[5] O. Chamberlain and E. Segrè, Phys. Rev. **87**, 81 (1952); J. B. Cladis, W. N. Hess, and B. J. Moyer, Phys. Rev. **87**, 425 (1952).

[6] G. F. Chew, Phys. Rev. **80**, 196 (1950); G. F. Chew and M. L. Goldberger, Phys. Rev. **87**, 778 (1952).

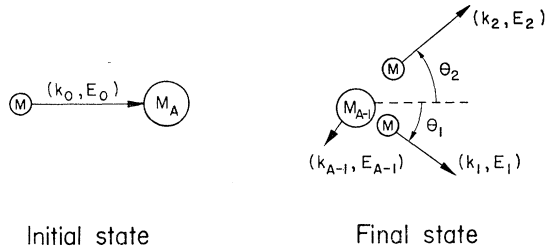

FIG. 1. The notation used in the text.

by assuming that the incoming proton collides with a single proton in the nucleus as if both particles were free. The observed angular correlation of the outgoing proton pairs differs from the one in free scattering (where the protons emerge under a definite angle which is nonrelativistically 90°) due to the fact that the nuclear protons are not at rest in the nucleus but have a momentum distribution. The momentum distributions estimated[7] on this basis from the Berkeley experiments are of a reasonable order of magnitude (see also Ref. 8).

After the development of the shell model, it became clear that not only the momentum distribution of the nuclear protons but also their separation energy distribution is an interesting quantity which is measurable by quasi-free scattering.[9] For a definite energy of the incoming particle, the summed energy spectrum of the emerging particle pairs is expected to show peaks at the separation energies corresponding to the various nuclear shells from which the protons can be ejected. Furthermore, the width of such a peak is related by the uncertainty principle to the lifetime of the hole left in the corresponding shell. Finally, by combined energy and angular selection of the outcoming particles, information on the momentum distributions of the protons in individual shells might be obtained. Experiments started in 1957 at Uppsala[10] indeed show these expected features.

Above 100 MeV, which is the lower incident energy limit considered in this paper, $(p, 2p)$ reactions of the type mentioned above have been performed at Chicago[11–13] using 460-MeV incident energy, at Harvard[14–16] with 160 MeV, at Harwell[17] with 155 MeV, at Orsay[18–20] with 150 MeV, and at Uppsala[10,11,21,22] with 185 MeV. Mainly, nuclei up to ^{40}Ca have been investigated. For heavier nuclei there exists as yet little information[13,15,20]; in this region both the energy differences between the shells and the cross sections become relatively small.

Until recently only experiments with incoming protons were considered. In principle the large mean free path of electrons in nuclear matter makes these particles preferable as projectiles.[23] Although these experiments are difficult to perform because of the smallness of electromagnetic cross sections, the shell structure in ^{12}C and ^{27}Al has recently been resolved by the Istituto Superiore di Sanità group working at Frascati[24]; quasi-free electron–proton scattering in ^{2}H, ^{3}H, and ^{3}He has been performed at Stanford[25,26] and Orsay.[27] In all these measurements the incident electrons had energies between 500 and 600 MeV.

The present article reviews the theory and the experimental results of the mentioned quasi-free processes. We show how to extract information on the nucleus from the measurements, but we do not go into experimental details nor into a systematic investigation of the meaning of the obtainable nuclear data. The discussion is in general limited to nuclei with $A \geq 4$.

In the next section the quasi-free scattering process is considered in more detail but still qualitatively; the various types of experiments which have been performed are briefly discussed, and a comparison with deuteron pick-up is made. The third section contains a quantitative formulation of the reaction problem and a discussion of the methods used for the evaluation

[7] P. A. Wolff, Phys. Rev. **87**, 434 (1952).
[8] J. M. Wilcox and B. J. Moyer, Phys. Rev. **99**, 875 (1955); J. G. McEwen, W. M. Gibson, and P. J. Duke, Phil. Mag. **2**, 231 (1957); L. S. Azhgirey, I. K. Vzorov, V. P. Zrelov, M. G. Mescheryakov, B. S. Neganov, R. M. Ryndin, and A. F. Shabudin, Nucl. Phys. **13**, 258 (1959).
[9] Th. A. J. Maris, P. Hillman, and H. Tyrén, Nucl. Phys. **7**, 1 (1958).
[10] H. Tyrén, Th. A. J. Maris, and P. Hillman, Nuovo Cimento **6**, 1507 (1957); H. Tyrén, P. Hillman, and Th. A. J. Maris, Nucl. Phys. **7**, 10 (1958); P. Hillman, H. Tyrén, and Th. A. J. Maris, Phys. Rev. Letters **5**, 107 (1960).
[11] H. Tyrén, P. Hillman, P. Isacsson, and Th. A. J. Maris, Proc. Intern. Conf. Nucl. Struct., Kingston (1960), p. 429.
[12] H. Tyrén, S. Kullander, and R. Ramachandran, Proc. Conf. Direct Interactions Nucl. Reaction Mech., Padua (1962), p. 1109.
[13] H. Tyrén, S. Kullander, O. Sundberg, R. Ramachandran, and P. Isaacson (private communication); see also Ref. 66.
[14] B. Gottschalk and K. Strauch, Phys. Rev. **120**, 1005 (1960).
[15] B. Gottschalk, K. Strauch, and K. H. Wang, Compt. Rend. Congr. Intern. Phys. Nucl., Paris (1964), Vol. 2, p. 324.
[16] B. Gottschalk, Ph.D. thesis, Harvard University (1962); B. Gottschalk, K. Strauch, and K. H. Wang (private communication).
[17] T. J. Gooding and H. G. Pugh, Nucl. Phys. **18**, 46 (1960); H. G. Pugh and K. F. Riley, Proc. Rutherford Jubilee Intern. Conf., Manchester (1961), p. 195.
[18] J. P. Garron, J. C. Jacmart, M. Riou, and C. Ruhla, J. Phys. Radium **22**, 622 (1961); J. P. Garron, J. C. Jacmart, M. Riou, C. Ruhla, J. Teillac, and K. Strauch, Nucl. Phys. **37**, 126 (1962).
[19] J. P. Garron, Ann. Phys. (Paris) **7**, 301 (1962).
[20] C. Ruhla, M. Riou, R. A. Ricci, M. Arditi, H. Doubre, J. C. Jacmart, M. Liu, and L. Valentin, Phys. Letters **10**, 326 (1964).
[21] G. Tibell, O. Sundberg, and U. Miklavžič, Phys. Letters **1**, 172 (1962); **2**, 100 (1962); G. Tibell, O. Sundberg, and U. Miklavžič, Proc. Conf. Direct Interaction Nucl. Reaction Mech., Padua (1962) 1134.
[22] G. Tibell, O. Sundberg, and P. U. Renberg, Arkiv Fysik **25**, 433 (1963).
[23] G. Jacob and Th. A. J. Maris, Proc. Rutherford Jubilee Intern. Conf., Manchester (1961), p. 153; G. Jacob and Th. A. J. Maris, Nucl. Phys. **31**, 139 (1962); **31**, 152 (1962).
[24] U. Almaldi, Jr., G. Campos Venuti, G. Cortellessa, G. Fronterotta, A. Reale, P. Salvadori, and P. Hillman, Phys. Rev. Letters **13**, 341 (1964); Compt. Rend. Congr. Intern. Phys. Nucl., Paris (1964), Vol. 2, p. 341; Atti Accad. Nazl. Lincei, Rend. Classe Sci. Fis. Mat. Nat. **38**, 499 (1965); and private communication.
[25] M. Croissiaux, Phys. Rev. **127**, 613 (1962).
[26] A. Johansson, Phys. Rev. **136**, B1030 (1964).
[27] P. Bounin, Ann. Phys. (Paris) **10**, 475 (1965).

of the expression found for the cross section. The fourth section gives some typical experimental and theoretical results and reviews the most interesting information so far obtained. In the fifth section more results for individual nuclei are given, and finally some concluding remarks are made.

Without an appreciable loss of continuity Secs. IIIA, IIIB, and V may be omitted, except for formulas (3.23) and (3.27) and the immediately following discussions. In order not to obscure the basic simplicity of the matter, we have tried to avoid those questions of formal or technical nature which up to now have not been fruitful for the subject.

II. QUALITATIVE DESCRIPTION

When a 200-MeV proton is scattered at an angle of the order of 45°, the transferred momentum corresponds to a reduced de Broglie wavelength of about 0.5 F. This is a rather small quantity compared to the average distance of 2 F between two neighboring nucleons in the nucleus. Taking also into account that very small momentum transfers to a nucleon in the nucleus are unlikely to cause excitation because of the exclusion principle, one may expect that the inelastic interaction of a high energy nucleon with a nucleus can crudely be described as a sequence of independent nucleon–nucleon collisions.[4] A quasi-free event corresponds in this picture to the case in which only one such collision has taken place.

In the following we denote the incoming proton, the nuclear proton to be knocked out and the two outgoing protons by the indices 0, 3, 1, and 2. The index A denotes the initial nucleus, and $(A-1)$ refers to the state of the final nucleus, which may have an energy located in the continuous part of the spectrum. The remaining notation used is shown in Fig. 1; $(\hbar\mathbf{k}_j, E_j/c)$ are energy momentum four vectors.

From its definition the separation energy of the ejected proton for a certain final state of the nucleus is

$$S=T_0-(T_1+T_2+T_{A-1}), \tag{2.1}$$

where T_j stands for a kinetic energy; the initial nucleus is supposed to be at rest. Energy momentum conservation gives

$$E_0+M_Ac^2=E_1+E_2+E_{A-1}, \tag{2.2}$$

$$\mathbf{k}_0=\mathbf{k}_1+\mathbf{k}_2+\mathbf{k}_{A-1}, \tag{2.3}$$

where

$$E_{A-1}=M_{A-1}c^2+E_{\text{exc}}+T_{A-1}, \tag{2.4}$$

E_{exc} being the excitation energy of the residual nucleus. From Eqs. (2.1), (2.2), and (2.4), it follows that this excitation energy equals the difference between the separation energies of the least bound proton and the ejected one.

We consider first the idealized situation in which the incoming proton interacts with only one nucleon which is moving in an ideal shell model nucleus. It is not difficult to see which corrections have to be applied to this model in order to make it more realistic; the application to electron scattering is also an easy matter. In this idealized case the separation energy of application to electron scattering is also a simple matter. In this idealized case the separation energy of the ejected proton and the recoil momentum of the residual nucleus have a simple physical meaning. The final nucleus has evidently a hole in the shell from which the proton was ejected, and the separation energy equals the (negative) energy of its single-particle state. Because the initial nucleus was at rest, the nuclear recoil momentum $\hbar\mathbf{k}_{A-1}$ equals $-\hbar\mathbf{k}_3$, i.e., minus the momentum the knocked out nucleon had in the nucleus. Consequently, the energy spectrum and recoil momentum distribution of the residual nucleus will directly correspond to the possible energies and momentum distributions of the single-particle states in the individual shells. These may therefore be determined from a measurement of the dependence of the number of proton pairs emerging from quasi-free collisions on the momenta $\hbar\mathbf{k}_1$ and $\hbar\mathbf{k}_2$.

Although several important modifications are necessary, the simple picture just given contains, in our opinion, the essential physics of the quasi-free process and motivates the use of these reactions for the investigation of nuclear structure.

In fact, the experimental energy spectra show peaks corresponding to the knocking out of nuclear protons from different shells and subshells, and the qualitative features of the momentum correlations of protons ejected from a shell agree well with the expected behavior of the corresponding wave function in momentum space.

Now the main corrections which have to be made to the above mentioned model will be discussed.[9] First we still consider the nucleus as having a perfect single-particle structure, but take into account the multiple collisions which the incoming and the two outgoing protons suffer in the nucleus. Then deviations from the single-particle structure are included.

A quasi-free event can be "spoiled" because the incoming particle or the two outgoing ones have inelastic interactions with other nucleons in the nucleus before, during, or after the quasi-free collision. By such multiple collisions either additional particles are ejected or at least extra excitations of the nucleus are caused. These events tend to blur the simple picture from which we started.

The cases in which the incoming proton interacts during the quasi-free collision with a third particle will be relatively rare if the de Broglie wavelength corresponding to the momentum transfer is sufficiently small and strong short-range correlations between nuclear nucleons are absent.[6] However, the multiple

collisions before and after the quasi-free event are important. As seen in the next section one may take these into account by introducing complex optical potentials for the incoming and outgoing protons. Either from experimental proton–nucleon total cross sections or from the optical potential obtained from elastic proton–nucleus scattering, the mean free path of a 150–400-MeV proton in nuclear matter may be estimated to be smaller than the radius of even a very light nucleus; it is therefore clear that in general multiple collisions will not be rare but will in fact occur more frequently than quasi-free ones. Thus one might fear that the measured energy spectrum and the correlation pattern of the outcoming proton pair mainly stem from protons which have suffered multiple collisions and therefore no longer reflect the single particle structure of the nucleus. The following circumstance saves the situation. Because of the large number of degrees of freedom available in the final states resulting from multiple collisions, the measured energies and momenta of a proton pair are distributed over the whole available energy and angular range and should therefore result in a rather smooth background in the measured energy spectrum of the residual nucleus. This background starts at the energy corresponding to the ground state of the residual nucleus and rises with excitation energy and atomic number. Superimposed on it one may expect to see the peaks caused by clean knock out collisions as long as any structure in the background does not become comparable with these peaks. This is also the general reason why the expected spectra are not very sensitively dependent on the perfect applicability of the Serber–Chew model[4,6] for quasi-free collisions.

Nevertheless, for the study of quasi-free scattering the multiple collisions are an unfavorable effect, decreasing the peak heights, increasing the background, and distorting the momentum correlation distributions. From the expected values of the mean free path of the incoming and outgoing protons, one may estimate that in this respect the optimum bombarding energy is about 400 MeV. The great advantage of $(e, e'p)$ over $(p, 2p)$ experiments is that in the former case only the absorption of one outgoing proton is of importance. The effect of multiple collisions on the experimental results, and the calculated corrections for specific nuclei are found in the following sections.

The extreme single-particle model is only a very approximate description of the nucleus; it predicts an energy spectrum with a small number of sharp peaks, whereas observed spectra are often rather complex and contain peaks of considerable width. We now discuss how these features may be qualitatively understood by taking deviations from the single-particle model into account.

A considerable amount of short-range nucleon–nucleon correlations would frequently lead to rearrangements in the residual nucleus[28,29] and, consequently, depress the number of quasi-free collisions. This effect has hardly been studied and should probably be taken into account by a momentum- and shell-dependent reduction factor to be applied to calculated cross sections. In practice, at present one is only able to obtain information on the low momentum part of the momentum distributions; for this region one would not expect the effect of short-range correlations and the resulting rearrangements to be very important, except perhaps for a nearly constant normalization factor.

The structure of the long-range nucleon–nucleon correlations, for example those described by configuration mixing and by a deformation of the nucleus, may, however, considerably influence the spectra obtained from quasi-free scattering processes in the upper shell. These spectra become less simple because of the splittings of the upper shell states and the complicated overlap of these states in the initial and final nucleus. In favorable cases fractional parentage coefficients might be estimated from experimental results[9,30,31]; the effect of deformations on the experimental results will be seen in ^{9}Be and in the $2s$–$1d$ shell nuclei.

Of special interest is the investigation of inner shell states, which up to now has been exclusively performed by quasi-free scattering experiments. The width of a peak in the energy spectrum corresponding to those states may be understood by considering the lifetime of the resulting hole state of the (highly excited) residual nucleus. If a proton has been ejected from an inner shell, the exclusion principle is no longer effective[32,33] in forbidding collisions which fill up the hole. The hole state may therefore have a short lifetime, and this causes a broadening of the peaks in the spectrum corresponding to inner shell states. The lifetimes of these states are expected to decrease with increasing number of particles in the shell above the one containing the hole.[34] If the lifetime becomes very small, the simple shell model description ceases to be useful for these states. The broadening effect has been clearly observed in the quasi-free spectra of inner shells and may constitute a limitation of the number of shells which can be investigated. For example, we see that the full width at half-height of the energy peak corresponding to the ejection of a proton out of the $1s$ shell rises from 3 MeV or less for ^{6}Li [as obtained from

[28] Discussion remarks of K. A. Brueckner and V. F. Weisskopf, Proc. Intern. Conf. Nucl. Optical Model, Tallahassee (1959), p. 143.
[29] D. R. Inglis, Nucl. Phys. **30**, 1 (1962).
[30] V. V. Balashov and A. N. Boyarkina, Nucl. Phys. **38**, 629 (1962); V. V. Balashov, A. N. Boyarkina, and I. Rotter, Nucl. Phys. **59**, 417 (1964).
[31] K. Dietrich, Phys. Letters **2**, 139 (1962).
[32] V. F. Weisskopf, Helv. Phys. Acta **23**, 187 (1950).
[33] L. C. Gomes, J. D. Walecka, and V. F. Weisskopf, Ann. Phys. (N.Y.) **3**, 241 (1958).
[34] Th. A. J. Maris, Proc. Conf. Direct Interaction Nucl. Reaction Mech., Padua (1962), p. 31.

$(p, 2p)$ experiments] to about 20 MeV for ^{27}Al [from $(e, e'p)$ experiments].

A state with a hole in the inner shell of a nucleus with nonzero total angular momentum (or isospin) should be split because of the coupling of the angular momenta (isospins) of the inner shell and the upper one. We will meet an indication of this splitting in the spectrum of ^{6}Li.

Turning now to the experimental side, we briefly comment on the types of quasi-free measurements which have been performed up to date. It is apparent from the discussion above that one must determine the momenta (i.e., energies and directions) of both outgoing particles, which therefore have to be detected in coincidence. The energies are measured by range telescopes, total energy absorbing crystals or magnets.

For a fixed energy of the incoming particle there are in the quasi-free experiment not less than five parameters which can be continuously varied, even disregarding polarizations; this should be compared with the two parameters in inelastic scattering. It is therefore essential to select measurements which are favorable from an experimental or theoretical point of view.

Until now the following types of experiments have been performed (see also Table I in Sec. IV):

Coplanar $(p, 2p)$ experiments,

(a) Experiments with no further restriction on the outgoing angles and energies.[17]

(b) Symmetric experiments, in which the two outgoing protons are selected to have equal energies and to emerge at equal angles with respect to the incoming beam.[10] The high symmetry makes the theoretical analysis of these experiments particularly simple.[35]

(c) Energy sharing experiments, in which the directions of the outgoing protons are kept fixed and the outgoing energies are varied.[14] Because, in contradistinction to case (b), a large part of the number of particle pairs entering the counters is used, these measurements are attractive from an experimental point of view.

Coplanar $(e, e'p)$ experiments,

(d) In the only experiments which have been performed at present for nuclei with $A \geq 4$, the incoming energy has been varied, with all other parameters fixed.[24]

Closing this section we compare the quasi-free scattering with the high energy deuteron pick-up reaction[36] in which also a nucleon is taken out of the nucleus. The following reasons lead one to expect that, compared with appropriately chosen quasi-free scattering at the same energy, deuteron pick-up emphasizes the upper shell more strongly.

(a) In deuteron pick-up, especially at higher energies, high momentum nucleons are snatched out of the nucleus,[37] and the nucleons of the upper shell have the largest average kinetic energy. In symmetric quasi-free scattering at about 45°, one is selecting low momentum nucleons which belong more to the inner nuclear shells.

(b) A strong absorption tends to locate the interactions at the nuclear surface, which consists predominantly of upper shell nucleons. The choice of equal energies of the two outgoing particles, as obtainable in quasi-free scattering, results in the smallest total absorption. In deuteron pick-up the distorted deuteron wave function in the nucleus corresponds to a neutron and a proton of greatly differing absolute momenta, resulting in an increase of absorption and reflection.[38]

For these reasons we think that at a given bombarding energy quasi-free scattering offers better possibilities than deuteron pick-up for the study of inner shells. The optimum energy for the investigation of these shells with quasi-free scattering is probably about 400 MeV. At such energies the nucleon to be picked up in deuteron pick-up must have a very high momentum, so that the cross section for this reaction becomes very small, and secondary processes become important. At present there seems to exist only one experiment[39] in which there is an indication of a pick-up from an inner shell, namely from the $1p$ shell in ^{19}F. In this case there are only three particles in the upper shell.

Although quasi-free scattering holds at present a near monopoly for inner shell investigations, this is of course in no way the case with respect to the upper shell. For this shell pick-up (and other) reactions, though accentuating different properties of the wavefunctions than the quasi-free experiments, are in general more practical because they do not require a coincidence technique and allow for higher resolutions.

III. QUANTITATIVE CONSIDERATIONS

In this section we give a somewhat naive but simple derivation of the relativistic cross section formula in the Distorted Wave Impulse Approximation (DWIA).[9,35,40] Although the same result may be obtained in a slightly more sophisticated manner, drastic approximations are anyhow unavoidable in order to reduce the number of degrees of freedom of the many-body problem under

[35] Th. A. J. Maris, Nucl. Phys. **9**, 577 (1958/59).

[36] K. Brueckner and W. Powell, Phys. Rev. **75**, 1274 (1949); J. Hadley and H. York, Phys. Rev. **80**, 345 (1950); W. Selove, Phys. Rev. **101**, 231 (1956); P. Radvanyi, J. Genin, and C. Detraz, Phys. Rev. **125**, 295 (1962); D. Bachelier, M. Bernas, I. Brissaud, C. Detraz, N. K. Ganguly, and P. Radvanyi, Phys. Letters **8**, 56 (1964).

[37] G. F. Chew and M. L. Goldberger, Phys. Rev. **77**, 470 (1950).

[38] L. R. B. Elton and L. C. Gomes, Phys. Rev. **105**, 1027 (1957).

[39] P. Radvanyi (private communication).

[40] T. Berggren and G. Jacob, Phys. Letters **1**, 258 (1962); T. Berggren and G. Jacob, Proc. Conf. Direct Interaction Nucl. Reaction Mech., Padua (1962), p. 33; T. Berggren and G. Jacob, Nucl. Phys. **47**, 481 (1963).

investigation to a manageable one (see the Introduction of Ref. 41). These approximations do not have a mathematical basis but only a physical one, and therefore, it seems natural to try to keep the derivation transparent from a physical point of view.

We first calculate the cross section in the Born approximation, in this way obtaining the general structure of the relevant matrix element with the correct kinematical factors, without being troubled by other complications. The improvement of the resulting expression to the DWIA is then a relatively simple matter; in the last part of this section, applications to some special cases are made.

Although our treatment is in general relativistic where fast particles are involved, for simplicity we use two-component wave functions for the nucleons. At the end it will be clear that a four-component description would not affect the derivation and the result appreciably.

A. The Cross Section in the Impulse Approximation

We start by listing some results from the theory of scattering.[42]

The process of interest is the transition from an initial state $|i\rangle$ consisting of a nucleus A and an incoming proton, to a final state $|f\rangle$ with a recoiling nucleus $(A-1)$ and two outgoing protons; for the symbols used see Fig. 1.

The general expression for the cross section is

$$\frac{d^9\sigma}{d^3k_1 d^3k_2 d^3k_{A-1}}=\frac{4\pi^2}{\hbar}\frac{E_0E_A}{F}|t_{fi}|^2\,\delta^3(\mathbf{k}_1+\mathbf{k}_2+\mathbf{k}_{A-1}-\mathbf{k}_0-\mathbf{k}_A)\,\delta(E_1+E_2+E_{A-1}-E_0-E_A), \tag{3.1}$$

where

$$F=c[(E_0E_A-\hbar^2c^2\mathbf{k}_0\cdot\mathbf{k}_A)^2-c^8M^2M_A{}^2]^{\frac{1}{2}}. \tag{3.2}$$

The matrix element t_{fi} is defined by

$$T_{fi}=\tfrac{1}{2}\pi^{-1}\delta^3(\mathbf{k}_1+\mathbf{k}_2+\mathbf{k}_{A-1}-\mathbf{k}_0-\mathbf{k}_A)\,t_{fi}, \tag{3.3}$$

with T_{fi} being related to the S matrix element by

$$S_{fi}=\delta_{fi}-2\pi i\delta(E_f-E_i)\,T_{fi}. \tag{3.4}$$

A perturbation expansion of T_{fi} is given by

$$T_{fi}=\langle f\,|\,V+V(E_i-H_0+i\epsilon)^{-1}V+\cdots\,|\,i\rangle. \tag{3.5}$$

In the first Born approximation, which we use as a starting point, one has for the quasi-free scattering process

$$T_{fi}=\langle f\,|\,V\,|\,i\rangle=\sum_{\alpha\neq\beta=0}^{A}\int\mathfrak{A}\{\exp(-i\mathbf{k}_2\cdot\mathbf{r}_0)s_2{}^+(0)t_p{}^+(0)\exp(-i\mathbf{k}_1\cdot\mathbf{r}_1)s_1{}^+(1)t_p{}^+(1)\psi^*_{A-1}(\mathbf{r},m,\mu)\}$$
$$\times V(\alpha,\beta)\mathfrak{A}\{\exp(i\mathbf{k}_0\cdot\mathbf{r}_0)s_0(0)t_p(0)\psi_A(\mathbf{r}_1,m_1,\mu_1;\mathbf{r},m,\mu)\}\,d^3r_0\,d^3r_1\,d^3r. \tag{3.6}$$

The symbols have the following meaning: $\mathfrak{A}\{\ \}$ is the antisymmetrization and normalization operator, $s(j)$ and $t(j)$ are spin and isospin wave functions of particle j, and m_j, μ_j are the corresponding variables in the nuclear wave functions; $V(\alpha,\beta)$ is the nucleon–nucleon interaction which is of course symmetric under the exchange of α and β. In scalar products summations over spin and isospin variables are understood.

Because of the antisymmetry of the wave functions, the terms under the sum of the right-hand side of Eq. (3.6) for different values of α and β are all equal and one may write

$$T_{fi}=\tfrac{1}{2}A(A+1)\int\mathfrak{A}\{\exp(-i\mathbf{k}_2\cdot\mathbf{r}_0)s_2{}^+(0)t_p{}^+(0)\exp(-i\mathbf{k}_1\cdot\mathbf{r}_1)s_1{}^+(1)t_p{}^+(1)\psi^*_{A-1}(\mathbf{r},m,\mu)\}$$
$$\times V(0,1)\mathfrak{A}\{\exp(i\mathbf{k}_0\cdot\mathbf{r}_0)s_0(0)t_p(0)\psi_A(\mathbf{r}_1,m_1,\mu_1;\mathbf{r},m,\mu)\}\,d^3r_0\,d^3r_1\,d^3r. \tag{3.7}$$

In practice the magnitudes of the momenta $\hbar\mathbf{k}_1$ and $\hbar\mathbf{k}_2$ are so large that they very seldom occur in the momentum distribution of the nuclear protons; thus each of the antisymmetrization operations will give rise to only two terms in the integrand of Eq. (3.7). Mathematically this follows from the fact that the rapidly oscillating functions $\exp(i\mathbf{k}_1\cdot\mathbf{r}_j)$ and $\exp(i\mathbf{k}_2\cdot\mathbf{r}_j)$ are practically orthogonal to the nuclear wave function with respect to integration over $\mathbf{r}_j$, and physically it is also clear that a nucleon pair can only obtain the very large momenta $\hbar\mathbf{k}_1$ and $\hbar\mathbf{k}_2$ through a direct interaction with a particle of high momentum. With the antisymmetric wave functions ψ_A and

[41] D. R. Hartree, Rept. Progr. Phys. **11**, 113 (1946/47).

[42] C. Møller, Kgl. Danske Videnskab. Selskab., Mat.-Fys. Medd. **23**, Nr. 1 (1945); W. Brenig and R. Haag, Fortschr. Physik **7**, 183 (1959); K. Nishijima, *Fundamental Particles* (W. A. Benjamin, Inc., New York, 1963); M. L. Goldberger and K. M. Watson, *Collision Theory* (John Wiley & Sons, Inc., New York, 1964).

ψ_{A-1} normalized to unity, one has thus

$$T_{fi}=\frac{A^{1/2}}{2(2\pi)^{9/2}}\int[\exp(-i\mathbf{k}_2\cdot\mathbf{r}_0)s_2^+(0)t_p^+(0)\exp(-i\mathbf{k}_1\cdot\mathbf{r}_1)s_1^+(1)t_p^+(1)$$
$$-\exp(-i\mathbf{k}_2\cdot\mathbf{r}_1)s_2^+(1)t_p^+(1)\exp(-i\mathbf{k}_1\cdot\mathbf{r}_0)s_1^+(0)t_p^+(0)]\psi^*_{A-1}(\mathbf{r},m,\mu)V(0,1)$$
$$\times[\exp(i\mathbf{k}_0\cdot\mathbf{r}_0)s_0(0)t_p(0)\psi_A(\mathbf{r}_1,m_1,\mu_1;\mathbf{r},m,\mu)-\exp(i\mathbf{k}_0\cdot\mathbf{r}_1)s_0(1)t_p(1)\psi_A(\mathbf{r}_0,m_0,\mu_0;\mathbf{r},m,\mu)]d^3r_0\,d^3r_1\,d^3r. \quad (3.8)$$

Because of charge conservation, μ_0 and μ_1 in ψ_A have the value corresponding to a proton. It is convenient to expand ψ_A in the following manner:

$$\psi_A(\mathbf{r}_1,m_1,\mu_1;\mathbf{r},m,\mu)=\frac{1}{(2\pi)^{\frac{3}{2}}}\sum_{n,j}\int\exp(i\mathbf{k}\cdot\mathbf{r}_1)s_n(1)t_j(1)g_A^{(n,j)}(\mathbf{k};\mathbf{r},m,\mu)\,d^3k. \quad (3.9)$$

Inserting (3.9) in (3.8), we obtain

$$T_{fi}=\int d^3k\sum_n A^{\frac{1}{2}}\int d^3r\psi^*_{A-1}(\mathbf{r},m,\mu)g^{(n)}{}_A(\mathbf{k};\mathbf{r},m,\mu)$$
$$\int d^3r_0\,d^3r_1\mathfrak{A}\{\exp(-i\mathbf{k}_2\cdot\mathbf{r}_0)s_2^+(0)t_p^+(0)\exp(-i\mathbf{k}_1\cdot\mathbf{r}_1)s_1^+(1)t_p^+(1)\}$$
$$\times V(0,1)\mathfrak{A}\{\exp(i\mathbf{k}_0\cdot\mathbf{r}_0)s_0(0)t_p(0)\exp(i\mathbf{k}\cdot\mathbf{r}_1)s_n(1)t_p(1)\}$$
$$=\sum_n\int d^3kA^{\frac{1}{2}}\int\psi^*_{A-1}(\mathbf{r},m,\mu)g_A^{(n)}(\mathbf{k};\mathbf{r},m,\mu)\,d^3r\langle\mathbf{k}_1,m_1;\mathbf{k}_2,m_2\mid V_{pp}\mid\mathbf{k}_0,m_0;\mathbf{k},n\rangle, \quad (3.10)$$

where $g_A^{(n)}=g_A^{(n,p)}$, t_p being a proton isospin function. Defining the function $M(1,2;0,3)$ by

$$M(1,2;0,3)\delta^3(\mathbf{k}_1+\mathbf{k}_2-\mathbf{k}_0-\mathbf{k}_3)=(E_1E_2)^{\frac{1}{2}}\langle\mathbf{k}_1,m_1;\mathbf{k}_2,m_2\mid V_{pp}\mid\mathbf{k}_0,m_0;\mathbf{k}_3,m_3\rangle(E_0E_3)^{\frac{1}{2}}, \quad (3.11)$$

we obtain, with $\mathbf{k}_3=\mathbf{k}_1+\mathbf{k}_2-\mathbf{k}_0$ and $E_3=(\hbar^2c^2k_3^2+M^2c^4)^{\frac{1}{2}}$,

$$T_{fi}=\sum_n A^{\frac{1}{2}}\int\psi^*_{A-1}(\mathbf{r},m,\mu)g_A^{(n)}(\mathbf{k}_3;\mathbf{r},m,\mu)d^3r(E_0E_1E_2E_3)^{-\frac{1}{2}}M(1,2;0,(\mathbf{k}_3,n)). \quad (3.12)$$

The total momentum conserving δ function which, according to Eq. (3.3), should occur in T_{fi} is contained in the integral of expression (3.12). To extract this δ function, we write the integral again in configuration space

$$\int\psi^*_{A-1}(\mathbf{r},m,\mu)g_A^{(n)}(\mathbf{k}_3;\mathbf{r},m,\mu)d^3r=\frac{1}{(2\pi)^{\frac{3}{2}}}s_n^+(1)t_p^+(1)\int\exp(-i\mathbf{k}_3\cdot\mathbf{r}_1)\psi^*_{A-1}(\mathbf{r},m,\mu)\psi_A(\mathbf{r}_1,m_1,\mu_1;\mathbf{r},m,\mu)\,d^3r_1\,d^3r. \quad (3.13)$$

Introducing as new variables the center of mass coordinates of the final nucleus $\mathbf{R}_{A-1}$ and the relative coordinates $\mathbf{x}_j=\mathbf{r}_j-\mathbf{R}_{A-1}$ ($j=1,2,\cdots,A-1$), one may write for the nuclear wave functions, assuming the initial nucleus to be at rest,

$$\psi^*_{A-1}(\mathbf{r},m,\mu)=[(A-1)^{\frac{1}{2}}/(2\pi)^{\frac{3}{2}}]\exp(-i\mathbf{k}_{A-1}\cdot\mathbf{R}_{A-1})\varphi^*_{A-1}(\mathbf{x},m,\mu)$$

and

$$\psi_A(\mathbf{r}_1,m_1,\mu_1;\mathbf{r},m,\mu)=[(A-1)^{\frac{1}{2}}/(2\pi)^{\frac{3}{2}}]\varphi_A(\mathbf{x}_1,m_1,\mu_1;\mathbf{x},m,\mu). \quad (3.14)$$

The so defined internal nuclear wave functions φ_A and φ_{A-1} contain, respectively, $(A-1)$ and $(A-2)$ space coordinates $\mathbf{x}_j$, with respect to which they are normalized to one.

Inserting Eqs. (3.14) in Eq. (3.13), we obtain after integration over $\mathbf{R}_{A-1}$

$$A^{\frac{1}{2}}\int\psi^*_{A-1}(\mathbf{r},m,\mu)g_A^{(n)}(\mathbf{k}_3;\mathbf{r},m,\mu)\,d^3r=g^{(n)}{}_{A-1,A}(\mathbf{k}_1+\mathbf{k}_2-\mathbf{k}_0)\delta^3(\mathbf{k}_1+\mathbf{k}_2-\mathbf{k}_0+\mathbf{k}_{A-1}), \quad (3.15)$$

where we have defined $g^{(n)}{}_{A-1,A}(\mathbf{k})$ by

$$g^{(n)}{}_{A-1,A}(\mathbf{k})=\frac{A^{\frac{1}{2}}}{(2\pi)^{\frac{3}{2}}}\int\exp(i\mathbf{k}\cdot\mathbf{x})\varphi^*_{A-1}(\mathbf{x},m,\mu)\varphi_A(\mathbf{x}_1,m_1,\mu_1;\mathbf{x},m,\mu)\,d^3x_1\,d^3x\,s_n^+(1)t_p^+(1). \quad (3.16)$$

In the case of a pure single-particle model, where the conservation of the center of mass momentum is neglected,

$|\, g^{(n)}{}_{A-1,A}(\mathbf{k})\,|^2$ is the momentum distribution the knocked-out proton had in the nucleus; in general it is the probability of finding a proton in a state of momentum $\hbar\mathbf{k}$ and spin state s_n, the rest of the initial nucleus being in the state ψ_{A-1}, i.e., in the internal state φ_{A-1} with momentum $-\hbar\mathbf{k}$.

From Eqs. (3.12), (3.15), and (3.3) we have

$$t_{fi}=2\pi\sum_n g^{(n)}{}_{A-1,A}(\mathbf{k}_3)\,(E_0E_1E_2E_3)^{-\frac{1}{2}}M(1,\,2;\,0,\,(\mathbf{k}_3,\,n)), \tag{3.17}$$

and consequently, for the cross section (3.1), after integrating over the coordinates of the undetected recoiling nucleus,

$$\frac{d^6\sigma}{d^3k_1d^3k_2}=\frac{(2\pi)^4}{\hbar}\frac{E_A}{F}(E_1E_2E_3)^{-1}\sum_n |\, M(1,\,2;\,0,\,(\mathbf{k}_3,\,n))\,|^2\,|\, g^{(n)}{}_{A-1,A}(\mathbf{k}_3)\,|^2\,\delta(E_1+E_2+E_{A-1}-E_0-E_A). \tag{3.18}$$

Using the relation

$$d^6\sigma/dE_1d\Omega_1dE_2d\Omega_2=[E_1E_2k_1k_2/(\hbar c)^4](d^6\sigma/d^3k_1d^3k_2) \tag{3.19}$$

and the value of F obtained from Eq. (3.2),

$$F=\hbar c^2k_0E_A, \tag{3.20}$$

Equation (3.18) may be written

$$\frac{d^6\sigma}{dE_1d\Omega_1dE_2d\Omega_2}=\left(\frac{2\pi}{\hbar c}\right)^4\frac{k_1k_2}{\hbar^2c^2k_0E_3}\sum_n |\, M(1,\,2;\,0,\,(\mathbf{k}_3,\,n))\,|^2\,|\, g^{(n)}{}_{A-1,A}(\mathbf{k}_3)\,|^2\,\delta(E_1+E_2+E_{A-1}-E_0-E_A). \tag{3.21}$$

Neglecting for the moment all off-energy shell effects, we can relate the function M of Eq. (3.21) to a cross section for the scattering process of free protons with initial momenta $\hbar\mathbf{k}_0$, $\hbar\mathbf{k}_3$ to the momenta $\hbar\mathbf{k}_1$, $\hbar\mathbf{k}_2$. Starting from the analog of Eq. (3.1) for this case, one finds for this cross section in the center of mass system, again using the Born approximation,

$$\frac{d\sigma^{fr}}{d\bar{\Omega}}(\bar{1},\,\bar{2};\,\bar{0},\,(\bar{\mathbf{k}}_3,\,n))=\frac{1}{4}\left(\frac{2\pi}{\hbar c}\right)^4\frac{1}{\bar{E}_0{}^2}\,|\, M(1,\,2;\,0,\,(\mathbf{k}_3,\,n))\,|^2, \tag{3.22}$$

where barred quantities are taken in the center of mass system. Eliminating M from Eqs. (3.21) and (3.22), we obtain

$$\frac{d^6\sigma}{dE_1d\Omega_1dE_2d\Omega_2}=\frac{4}{(\hbar c)^2}\frac{k_1k_2\bar{E}_0{}^2}{k_0E_3}\sum_n |\, g^{(n)}{}_{A-1,A}(\mathbf{k}_3)\,|^2\frac{d\sigma^{fr}}{d\bar{\Omega}}(\bar{1},\,\bar{2};\,\bar{0},\,(\bar{\mathbf{k}}_3,\,n))\,\delta(E_1+E_2+E_{A-1}-E_0-E_A). \tag{3.23}$$

In expressing the quasi-free proton–proton scattering matrix element by the free proton–proton cross section, we have neglected the fact that the momenta of the quasi-free matrix element do not occur in the free scattering because of the difference in energy conservation between the two cases. This difference is caused by the nonzero value of the separation energy in the quasi-free scattering and by the fact that in this case the recoiling nucleus has a smaller kinetic energy than the recoiling proton with the same momentum in the free scattering. This results in a certain arbitrariness; instead of eliminating the function M from Eqs. (3.21) and (3.22) one could, for instance, also have directly eliminated the matrix element of V_{pp} occurring in expression (3.11). Furthermore, there is an uncertainty for which momentum values to take the free cross section. Fortunately, these uncertainties, and therefore probably also the associated errors, amount only to a few percent as long as one considers quasi-free processes for which the equivalent free proton–proton scattering corresponds to a bombarding energy in the laboratory system between 150 and 400 MeV, where the cross section is nearly energy and angle independent.[43] In our expressions we have defined the equivalent free scattering by the two outgoing momenta $\hbar\mathbf{k}_1$ and $\hbar\mathbf{k}_2$; slightly different formulae are obtained for other definitions.

Expression (3.23) has a very simple interpretation. Except for some kinematical factors, the cross section for a process in which the two final protons have momenta $\hbar\mathbf{k}_1$ and $\hbar\mathbf{k}_2$ and the final nucleus is in the state ψ_{A-1} is given by the product of a free proton–proton cross section with the probability to find a proton in the initial nucleus in a state with the momentum demanded by momentum conservation, the rest of the nucleus being in the required final state. If the initial and final nuclei are polarized, the free cross sections for polarized protons will in general enter in Eq. (3.23). For unpolarized nuclei, averaging over the initial spin states m_A and summing over the final

[43] V. S. Barashenkov and V. M. Maltsev, Fortschr. Physik **9**, 549 (1961).

ones m_{A-1}, one may make the replacement[9]

$$\sum_{m_{A-1},m_A}\sum_n |\, g^{(n)}{}_{m_{A-1},m_A}(\mathbf{k}_3)\,|^2 \frac{d\sigma^{fr}}{d\bar{\Omega}}(\bar{1},\bar{2};\bar{0},(\bar{\mathbf{k}}_3,n))$$

$$=\frac{d\sigma^{fr}}{d\bar{\Omega}}(\bar{1},\bar{2};\bar{0},\bar{3}_u)\sum_{m_{A-1},m_A}|\, g_{m_{A-1},m_A}(\mathbf{k}_3)\,|^2,$$

where $(d\sigma^{fr}/d\bar{\Omega})(\bar{1},\bar{2};\bar{0},\bar{3}_u)$ is the cross section for the case in which proton 3 is unpolarized, the remaining ones having the spin orientation selected by the experiment. As is seen later this does not hold anymore when distortion is taken into account.

Up to now we have used the Born approximation both for the quasi-free and for the free scattering. In reality our final formula is more accurate than this approximation would suggest. The Born approximation in the quasi-free scattering introduces two types of errors. It neglects the possibility of obtaining the final state through various intermediate nuclear states, and it gives the proton–proton matrix element badly even for free scattering. At the present energies the last error is by far the most serious one. In the present so-called impulse approximation,[6] we have largely eliminated this error by expressing the proton–proton matrix element directly in terms of an experimental quantity; in this matrix element we have still neglected off energy shell effects. In contradistinction to the Born approximation, however, the impulse approximation gives the exact cross section for the limiting case of a shell model nucleus with a common potential which is negligible compared to the kinetic energies of the incoming and emerging protons.

B. The Distorted Wave Impulse Approximation

In order to take the multiple scattering of the incoming and the two outgoing protons into account, we consider the corresponding plane waves to be distorted by optical potentials which are taken as spin independent for simplicity. In general different potentials have to be taken for each of these protons, mainly because they have different energies. Neglecting the contribution of the knocked out particle to the optical potential for the incoming proton, we write the distorted plane waves as

$$\exp(i\mathbf{k}_0\cdot\mathbf{r}_j)D_0(\mathbf{r}_j-\mathbf{R}_{A-1}),$$

$$\exp(-i\mathbf{k}_1\cdot\mathbf{r}_j)D_1(\mathbf{r}_j-\mathbf{R}_{A-1}),$$

and

$$\exp(-i\mathbf{k}_2\cdot\mathbf{r}_j)D_2(\mathbf{r}_j-\mathbf{R}_{A-1}) \qquad (j=0,1), \quad (3.24)$$

respectively; the D's are slowly varying functions compared to the plane waves and go to unity for values of the argument larger than the nuclear radius.

As in the preceding subsection we start using the Born approximation. In formula (3.6) the plane waves are to be replaced by the functions (3.24), and Eq. (3.8) becomes

$$T_{fi}=\frac{A^{1/2}}{2(2\pi)^{9/2}}\int[\exp(-i\mathbf{k}_2\cdot\mathbf{r}_0)D_2(\mathbf{r}_0-\mathbf{R}_{A-1})s_2{}^+(0)t_p{}^+(0)\exp(-i\mathbf{k}_1\cdot\mathbf{r}_1)D_1(\mathbf{r}_1-\mathbf{R}_{A-1})s_1{}^+(1)t_p{}^+(1)$$
$$-\exp(-i\mathbf{k}_2\cdot\mathbf{r}_1)D_2(\mathbf{r}_1-\mathbf{R}_{A-1})s_2{}^+(1)t_p{}^+(1)\exp(-i\mathbf{k}_1\cdot\mathbf{r}_0)D_1(\mathbf{r}_0-\mathbf{R}_{A-1})s_1{}^+(0)t_p{}^+(0)]\psi^*_{A-1}(\mathbf{r},m,\mu)V(0,1)$$
$$\times[\exp(i\mathbf{k}_0\cdot\mathbf{r}_0)D_0(\mathbf{r}_0-\mathbf{R}_{A-1})s_0(0)t_p(0)\psi_A(\mathbf{r}_1,m_1,\mu_1;\mathbf{r},m,\mu)$$
$$-\exp(i\mathbf{k}_0\cdot\mathbf{r}_1)D_0(\mathbf{r}_1-\mathbf{R}_{A-1})s_0(1)t_p(1)\psi_A(\mathbf{r}_0,m_0,\mu_0;\mathbf{r},m,\mu)]\,d^3r_0\,d^3r_1\,d^3r. \quad (3.25)$$

We now assume that the relative change of the distorting functions is small over a distance of the order of the range of the potential $V(0,1)$; we may then suitably replace $\mathbf{r}_0$ by $\mathbf{r}_1$ and vice-versa in the D's to obtain formula (3.8) with the replacement of ψ_A by the function

$$\psi'_A(\mathbf{r}_j,m_j,\mu_j;\mathbf{r},m,\mu)=D_0(\mathbf{r}_j-\mathbf{R}_{A-1})D_1(\mathbf{r}_j-\mathbf{R}_{A-1})D_2(\mathbf{r}_j-\mathbf{R}_{A-1})\psi_A(\mathbf{r}_j,m_j,\mu_j;\mathbf{r},m,\mu) \qquad (j=0,1). \quad (3.26)$$

From here on the treatment leading from Eq. (3.8) to Eq. (3.23) is completely applicable if the replacement $\psi_A\to\psi'_A$ is made everywhere. Finally we obtain instead of Eq. (3.23)

$$\frac{d^6\sigma}{dE_1d\Omega_1dE_2d\Omega_2}=\frac{4}{(\hbar c)^2}\frac{k_1k_2\bar{E}_0{}^2}{k_0E_3}\sum_n |\, g'^{(n)}{}_{A-1,A}(\mathbf{k}_3)\,|^2\frac{d\sigma^{fr}}{d\bar{\Omega}}(\bar{1},\bar{2};0,(\bar{\mathbf{k}}_3,n))\,\delta(E_1+E_2+E_{A-1}-E_0-E_A), \quad (3.27)$$

with

$$g'^{(n)}{}_{A-1,A}(\mathbf{k})=\frac{A^{\frac{1}{2}}}{(2\pi)^{\frac{3}{2}}}\int\exp(i\mathbf{k}\cdot\mathbf{x}_1)\varphi^*_{A-1}(\mathbf{x},m,\mu)\varphi_A(\mathbf{x}_1,m_1,\mu_1;\mathbf{x},m,\mu)D_0(\mathbf{x}_1)D_1(\mathbf{x}_1)D_2(\mathbf{x}_1)\,d^3x_1\,d^3x\,s_n{}^+(1)t_p{}^+(1).$$

We refer to the quantity $|\, g'^{(n)}{}_{A-1,A}\,|^2$ as the "distorted momentum distribution," having in mind that the momentum distribution $|\, g^{(n)}{}_{A-1,A}\,|^2$ as defined in Eq. (3.16) is modified by the distortions D of the plane waves of the incoming and emerging protons. This corresponds to the fact that the protons before and after the collision are scattered in the nucleus and that therefore the momentum distribution, naively deduced with the help of momentum conservation from the asymptotic momenta of the protons, does not corre-

spond exactly to the actual momentum distribution the knocked out proton had in the nucleus.

From this picture it is also clear that the matrix element of $V(0, 1)$ which contributes in the actual scattering is not only the one between proton states with the asymptotic momenta. If, however, the momentum dependence of $V(0, 1)$ is not very strong, one may neglect this momentum spread and calculate the matrix element with the asymptotic values. This corresponds partly to our assumption in the derivation that the distortion does not change much over the range of $V(0, 1)$. In expressing an off energy shell matrix element of $V(0, 1)$ in terms of an experimental cross section, we introduce anyhow a certain arbitrariness in the choice of this cross section, which again demands a smooth momentum dependence of $V(0, 1)$.

In the case of $(p, 2p)$ scattering, the above mentioned uncertainties are probably unimportant, as the proton–proton cross section varies very little[43] with energy and angle in the 150–400-MeV region. For quasi-free electron–proton scattering this is no longer true, and a simple approximation of the type discussed above, in which a measurable free cross section is directly used, may be good only for special choices of the geometry in the experiment.[23]

Exhibiting the nuclear magnetic quantum numbers, the term

$$\sum_n |\, g'^{(n)}{}_{A-1,A}\,|^2\,(d\sigma^{fr}/d\bar{\Omega})\,(\bar{1},\,\bar{2};\,\bar{0},\,(\bar{\mathbf{k}}_3,\,n))$$

in Eq. (3.27) is equal to

$$\sum_n |\, g'^{(n)}{}_{m_{A-1},m_A}\,|^2$$

times the corresponding matrix element for free scattering on a proton with the normalized spin wave function

$$\sum_n g'^{(n)}{}_{m_{A-1},m_A} s_n \Big(\sum_n |\, g'^{(n)}{}_{m_{A-1},m_A}\,|^2\Big)^{-\frac{1}{2}}. \tag{3.28}$$

Quantizing the spin in the z direction, the polarization vector of such a proton is given by[35]

$$\mathbf{P}_{m_{A-1},m_A}=\frac{\mathrm{Re}\,(g'^{*(+)}{}_{m_{A-1},m_A}g'^{(-)}{}_{m_{A-1},m_A});\,\mathrm{Im}\,(g'^{*(+)}{}_{m_{A-1},m_A}g'^{(-)}{}_{m_{A-1},m_A});\,(|\,g'^{(+)}{}_{m_{A-1},m_A}\,|^2-|\,g'^{(-)}{}_{m_{A-1},m_A}\,|^2)}{\sum_n |\,g'^{(n)}{}_{m_{A-1},m_A}\,|^2}. \tag{3.29}$$

Likewise in the case of unpolarized nuclei, averaging over initial nuclear spin orientations and summing over the final ones shows that the equivalent free proton–proton cross section is the one for scattering on protons with the polarization vector

$$\mathbf{P}=\frac{\mathrm{Re}\,(\sum_{m_{A-1},m_A} g'^{*(+)}{}_{m_{A-1},m_A}g'^{(-)}{}_{m_{A-1},m_A});\,\mathrm{Im}\,(\sum_{m_{A-1},m_A} g'^{*(+)}{}_{m_{A-1},m_A}g'^{(-)}{}_{m_{A-1},m_A});\,\sum_{m_{A-1},m_A}(|\,g'^{(+)}{}_{m_{A-1},m_A}\,|^2-|\,g'^{(-)}{}_{m_{A-1},m_A}\,|^2)}{\sum_{m_{A-1},m_A}\sum_n |\,g'^{(n)}{}_{m_{A-1},m_A}\,|^2} \tag{3.30}$$

In case there exists a plane of mirror symmetry, $\mathbf{P}$ is perpendicular to it.

For unpolarized nuclei the cross section may therefore be written

$$\frac{d^6\sigma}{dE_1 d\Omega_1 dE_2 d\Omega_2}\;\frac{4}{(\hbar c)^2}\frac{k_1 k_2 \bar{E}_0^2}{k_0 E_3}\frac{d\sigma^{fr}}{d\bar{\Omega}}(\bar{1},\,\bar{2};\,\bar{0},\,\bar{3}_p)\frac{1}{2J_A+1}\sum_{m_{A-1},m_A}\sum_n |\,g'^{(n)}{}_{m_{A-1},m_A}(\mathbf{k}_3)\,|^2\,\delta(E_1+E_2+E_{A-1}-E_0-E_A), \tag{3.31}$$

in which $(d\sigma^{fr}/d\bar{\Omega})\,(\bar{1},\,\bar{2};\,\bar{0},\,\bar{3}_p)$ is the experimental cross section in the center of mass system for scattering of protons on protons with the polarization vector $\mathbf{P}$.

C. Special Cases

As the kinematical factors and the proton–proton cross sections occurring in expression (3.27) are slowly varying functions of $\mathbf{k}_3$, the shape of the correlation cross sections is governed by the value of the distorted momentum distribution

$$\sum |\,g'\,|^2=(2J_A+1)^{-1}\sum_{m_{A-1},m_A}\sum_n |\,g'^{(n)}{}_{m_{A-1},m_A}(\mathbf{k}_3)\,|^2,$$

which is investigated in the present subsection.

To obtain an idea of this function one may first neglect the distortion. In the single-particle shell model, which is a good approximation for quasi-free scattering on a filled shell, $\sum |\,g'\,|^2$ is simply the momentum density distribution of this shell. For a harmonic oscillator potential the momentum density distribution of a shell differs only by a scale transformation from its density distribution in space. For other potentials both distributions have still several characteristics in common. Only s shells have nonvanishing zero momentum components, and in fact their densities are peaked at the origin, where the densities of the other shells have a minimum. The higher is the angular momentum in a shell, the further away from the origin the first maximum tends to be located. For any other model of the nucleus, as for example for the cluster model,[44]

[44] K. Wildermuth and Th. Kanellopoulos, Nucl. Phys. **7**, 150 (1958); K. Wildermuth and Th. Kanellopoulos, CERN Report 59-23 (1959).

one may easily show from the definition (3.16) that the undistorted momentum distributions can still only have nonvanishing values at the origin for angular momenta of the initial and final nucleus differing by $\frac{1}{2}$. All other distributions have a minimum at the origin, which is also true for the case of a different parity of the initial and final nuclei.[45] The distortion will more or less fill in these minima; it turns out in practice that a minimum resulting from a parity difference is more stable than one caused only by a nonzero angular momentum; for instance, the minimum for a p-state under similar circumstances will tend to be less filled in by the distortion than the one for a d-state.

Another instructive extreme is the case of very large absorption.[46] In this case the region in the nucleus where interactions leading to quasi-free scattering can occur is very limited and depends on the geometry of the experiment. If, for example, one considers approximately coplanar scattering with not too small an angle between the two outgoing proton momenta, the effective interaction region consists of two pole caps at the end of the nuclear diameter orthogonal to the scattering plane. One has now a situation analogous to the one in classical optics in which there are two coherent light sources. An interference pattern orthogonal to the scattering plane is expected; in the scattering plane a maximum or minimum should occur depending on the mirror-parity of the single-particle overlap integral. Comparing these distributions with the undistorted ones, one finds that the remark made at the end of the preceding paragraph applies. Experimentally, noncoplanar quasi-free scattering has not yet systematically been investigated.

For more general cases in which the absorption is neither extremely strong nor negligible, g'_{m_{A-1},m_A} may be found from Eq. (3.27). In this general case the distorting functions D have been determined using a complex optical potential, calculated from elastic scattering or from the nucleon–nucleon forward scattering amplitude.[47]

At the energies being considered in this paper, it seems to be most practical to calculate the distorted waves with the WKB (semiclassical) method (see, for example, Ref. 48). An elaborate phase-shift analysis[49,50] is not in the spirit of the present experiments, in which approximately sharp momenta but many angular momenta of the particles are involved. Already the error made in the phase-shift analysis by the necessary cutoff of the angular momentum value is of the same order of magnitude as the error of the WKB method.[51]

In the relativistic semiclassical method, the expressions for the D's are given by

$$D_0(\mathbf{r}) = \exp\left(-i\frac{E_0}{\hbar^2c^2k_0}\int_{-\infty}^{\mathbf{r}} V_0(\mathbf{r}')\,ds_0\right)$$

$$D_j(\mathbf{r}) = \exp\left(-i\frac{E_j}{\hbar^2c^2k_j}\int_{\mathbf{r}}^{\infty} V_j(\mathbf{r}')\,ds_j\right) \qquad (j=1,2), \tag{3.32}$$

where the V's are the complex optical potentials for the three particles and the integrations have to be performed along their classical paths.

Even for simple final and initial wavefunctions, the calculations of the distortions and the subsequent integrations necessary to calculate g' are not easy to do by hand. The general effect of the distorting exponentials (3.32) is to introduce additional real and imaginary momentum components. The former mainly smear out the angular distributions, and the latter decrease the intensity. This decrease may be by a considerable factor and can be crudely estimated for a specific nucleus and shell by mean free path considerations, as was already indicated in Sec. II.

With one exception[52] all detailed calculations of Eq. (3.31) have been performed for the symmetric coplanar scattering of unpolarized nucleons on unpolarized nuclei not observing final polarizations (see Table II in Sec. IV). For this case expression (3.27) simplifies to[35,40]

$$\frac{d^6\sigma}{dE_1d\Omega_1dE_2d\Omega_2} = \frac{4}{(\hbar c)^2}\frac{k^2}{k_0}\frac{\hbar^2c^2k^2\sin^2\theta+M^2c^4}{[\hbar^2c^2(2k\cos\theta-k_0)^2+M^2c^4]^{\frac{1}{2}}}\frac{d\sigma^{fr}}{d\bar{\Omega}}\frac{1}{2J_A+1}$$
$$\times\sum_{m_{A-1},m_A}\sum_n |\,g'^{(n)}_{m_{A-1},m_A}(\mathbf{k}_1+\mathbf{k}_2-\mathbf{k}_0)\,|^2\,\delta(2E+E_{A-1}-E_0-E_A). \tag{3.33}$$

Because there are two planes of mirror symmetry to which the effective polarization vector (3.30) of the knocked out nucleon has to be orthogonal, this vector vanishes and accordingly the cross section $d\sigma^{fr}/d\bar{\Omega}$ in Eq (3.33) is for unpolarized nucleons. This center of

[45] T. Berggren, G. E. Brown, and G. Jacob, Phys. Letters **1**, 88 (1962).

[46] G. Jacob and Th. A. J. Maris, Proc. Intern. Conf. Nucl. Struct., Kingston (1960), p. 433; G. Jacob and Th. A. J. Maris, Nucl. Phys. **20**, 440 (1960).

[47] K. M. Watson, Phys. Rev. **89**, 575 (1953); A. K. Kerman, H. McManus, and R. M. Thaler, Ann. Phys. (N.Y.) **8**, 551 (1959).

[48] L. D. Landau and E. M. Lifshitz, *Quantum Mechanics* (Pergamon Press, Inc., New York, 1958), p. 181; G. P. McCauley and G. E. Brown, Proc. Phys. Soc. (London) **71**, 893 (1958).

[49] K. L. Lim and I. E. McCarthy, Phys. Rev. Letters **10**, 529 (1963); K. L. Lim and I. E. McCarthy, Phys. Rev. **133**, B1006 (1964).

[50] D. F. Jackson and T. Berggren, Nucl. Phys. **62**, 353 (1965).

[51] T. Berggren (private communication).

[52] K. F. Riley, Nucl. Phys. **13**, 407 (1959); K. F. Riley, H. G. Pugh, and T. J. Gooding, Nucl. Phys. **18**, 65 (1960).

TABLE I. Quasi-free scattering experiments with incident energies larger than 100 MeV on nuclei with $A \geqslant 4$.

Group	Type of experiment	Energies	Nuclei investigated
Chicago (Refs. 11–13)	symmetric $(p, 2p)$	460 MeV	He, ^{6}Li, ^{7}Li, Be, ^{10}B, ^{11}B, C, N, O, Al, Si, P, S, A, Ca, V, Co
Rome (Ref. 24)	asymmetric $(e, e'p)$	500–600 MeV	Be, C, Al, S
Harvard (Refs. 14–16)	energy sharing $(p, 2p)$	160 MeV	^{6}Li, ^{7}Li, Be, ^{10}B, ^{11}B, C, N, O, F, Na, Mg, Al, Si, S, Cl, K, Ca, Sc, V, Co, Ni
Harwell (Ref. 17)	coplanar $(p, 2p)$	155 MeV	C; preliminary but not confirmed results on Li, Be, O, F, Na, Al, Si, P, S, Cl, Ca
Orsay (Refs. 18–20)	symmetric $(p, 2p)$	150 MeV	^{6}Li, ^{7}Li, Be, ^{10}B, ^{11}B, C, Ca, Sc, Ti, V, Cr, Mn, Fe, Ni, As
Uppsala (Refs. 10, 11, 21, 22)	symmetric $(p, 2p)$	185 MeV	He, ^{6}Li, ^{7}Li, Be, ^{10}B, ^{11}B, C, N, O, Na, Mg, Al, Si, P, Ca

mass cross section has to be taken at an angle of 90° and at an energy

$$\bar{E}_0=(\hbar^2c^2k^2\sin^2\theta+M^2c^4)^{\frac{1}{2}};$$

$$k^2=k_1^2=k_2^2, \qquad \theta=\theta_1=\theta_2, \qquad E=E_1=E_2.$$

Finally, a few words on quasi-free electron–proton scattering,[23] which has recently been performed on complex nuclei.[24] To avoid the problems introduced by the fast variation of the Coulomb-scattering matrix element with the momenta of the particles involved [see the discussion following expression (3.27)], the calculations are performed for fixed momenta of the electron, taking the variation of the momentum of the emerging proton approximately orthogonal to the scattering plane (for coplanar scattering see Ref. 53). The cross section for this process is given by[23]

$$\frac{d^6\sigma}{dE_e d\Omega_e dE_p d\Omega_p}$$

$$=(E_p^2-1)^{\frac{1}{2}}(1+2E_0\sin^2\tfrac{1}{2}\theta_e)\frac{d\sigma^{fr}}{d\Omega_e}\frac{1}{2J_A+1}$$

$$\times\sum_{m_{A-1},m_A}\sum_n|\,g'^{(n)}{}_{m_{A-1},m_A}(\mathbf{k}_e+\mathbf{k}_p-\mathbf{k}_0)\,|^2$$

$$\times\delta(E_e+E_p+E_{A-1}-E_0-E_A), \qquad (3.34)$$

where the indices 0, e, and p refer, respectively, to the incoming and outgoing electrons and to the outgoing proton; the rest mass of the electron has been neglected and all quantities have been expressed in units of $\hbar$, c and the proton mass M. The distorted momentum distribution $\sum|g'|^2$ has been evaluated for incoming and outgoing electrons of at least several hundred MeV and outgoing protons of an energy between 150 and 400 MeV. The general result is that the shape of the angular correlations is practically unchanged by the multiple scattering of the emerging proton, but that its magnitude is reduced by a factor of order one (see Fig. 14 of the next section). This is in agreement with the qualitative expectation of Sec. II.

IV. SOME EXAMPLES AND SURVEY OF RESULTS

In this section we discuss a few examples showing the main features of the experimental results and make a comparison with calculations.

A. Experimental Results

The experimental work which has been done up to now is summarized in Table I; for more experimental details see Table 1.3 in Ref. 22. Up to now virtually all of the quasi-free experiments have been performed with incident protons. The few existing electron experiments seem however to show their potential advantage for the investigation of inner shells, as expected from the large mean free path of electrons in nuclear matter.

The energy spectrum and angular correlation obtained in the symmetric quasi-free proton–proton scattering of 460-MeV protons on ^{4}He is shown in Fig. 2.

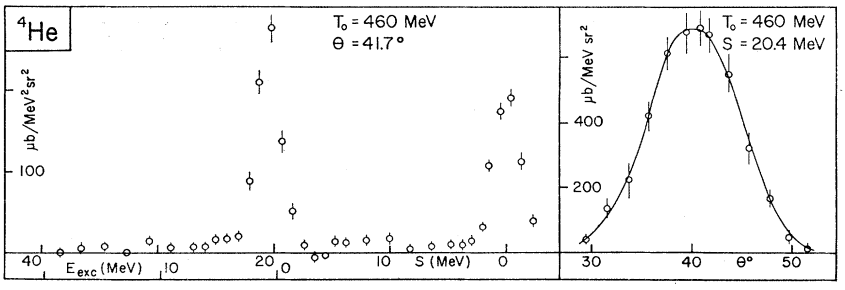

FIG. 2. Energy spectrum and angular correlation[13] for the ^{4}He$(p, 2p)^3$H reaction (symmetric case). The peak at zero separation energy results from scattering on free target protons.

[53] J. Potter, Nucl. Phys. **45**, 33 (1963).

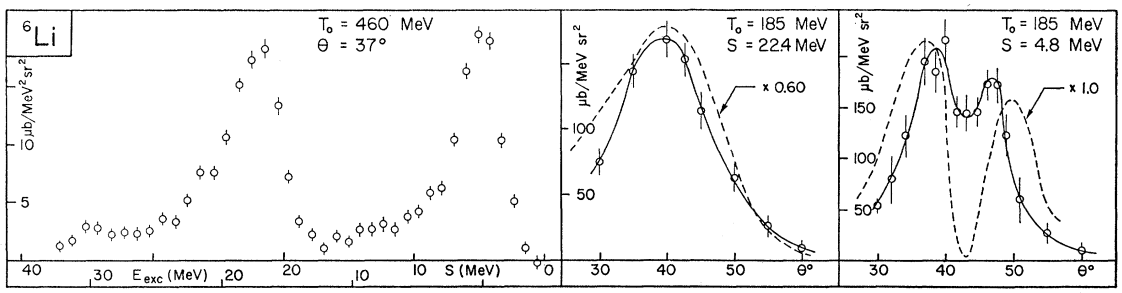

FIG. 3. Energy spectrum[18] and angular correlations[22] for the reaction ^{6}Li$(p, 2p)^5$He (symmetric case). The dotted lines are calculated results[57] multiplied by the indicated factors.

(At the cost of some uniformity we have tried to represent the experimental results in a way similar to the one of the original publications; absolute values for the cross section of the energy sharing experiments are given in the references 14–16.) At zero separation energy one sees the peak corresponding to the scattering on free protons which were present in the target; because these protons are at rest, they cause a relatively high contribution for certain angles. Only one group of protons is knocked out of the ^{4}He nucleus, and the angular correlation with its maximum at the angle for scattering on free protons at rest, corrected for the separation energy (which from now on is called the "free" scattering angle), clearly corresponds to the momentum distribution of an s proton. The width of the peak in the energy spectrum equals the experimental energy resolution. The separation energy is about 20 MeV, which means that the residual ^{3}H nucleus is left in its ground state or in a slightly excited state. For this very light nucleus, it is surprising that the results are, at least qualitatively, the ones predicted by the shell model. The measurements clearly support the soundness of the general interpretation described in the preceding sections.

Figures 3–6 show the energy spectra and angular correlation curves for quasi-free scattering experiments [symmetric $(p, 2p)$ and nonsymmetric $(e, e'p)$] on some $1p$ shell nuclei at the energies indicated in the figures. The dotted lines in the angular correlation curves represent calculated results, to which we will come back later.

In the framework of the shell model, the ^{6}Li nucleus is an alpha-particle with one proton–neutron pair added in the $1p$ shell; this picture is clearly in agreement with the energy spectrum and the angular correlations given in Fig. 3. The two added particles have increased the separation energy of the $1s$ proton to 22 MeV and decreased the cross section for the quasi-free process because of the absorption. The spectrum also shows the group of protons from the $1p$ shell with 4.8-MeV separation energy.

The angular correlation curves confirm the above assignments. Compared to other cases, the two maxima in the $1p$ correlation curve are relatively high and rather close to each other, which causes the minimum at about 42° to be shallow. This is qualitatively understandable from the low separation energy of the $1p$ proton, which causes a long exponential tail in its single particle wave function, thus reducing the absorption and also introducing additional low momentum components.

Because the ground state of ^{6}Li has $J=1$, one would expect the hole in the $1s$ shell to couple with the $1p$ shell to give states with $J=\frac{3}{2}$ and $J=\frac{1}{2}$, occurring with a probability ratio of 2:1. Speculating that the deformation of the $1s$ peak in Fig. 3 is caused by this splitting, one would find that the state with an antiparallel coupling of the two angular momenta has an energy of about 2 MeV lower than the state with a parallel coupling.

Also the energy spectrum and angular correlations for ^{12}C, given in Fig. 4, agree qualitatively with the shell model expectations. The $1s$ proton is bound by 36 MeV, and the hole state has a width of about 13 MeV, evidently being already quite short lived. The knocking out of a $1p$ proton is expected to lead to the $\frac{1}{2}^-$ ground state and to the $\frac{3}{2}^-$, 2.13-MeV first excited state[54] of ^{11}B. The intensity ratio for intermediate coupling is expected to lie between 0:1 and 1:2, the extreme values being the ones for pure j–j and L–S coupling. The splitting is clearly indicated in Fig. 4, the mentioned ratio being about 1:3.

For comparison Fig. 5 shows the spectrum of ^{12}C from electron scattering with the geometry indicated in the figure. This is the first experiment of this type on a complex nucleus; the resolution is not yet high, but the qualitative agreement with the $(p, 2p)$ result is evident. Also the number of events agrees well with the expected one,[55] assuming the quasi-free scattering model.

Basically the same features as in ^{12}C are shown by the $(p, 2p)$ results for ^{16}O in Fig. 6. The separation energy and the width of the $1s$ peak have increased still more, as expected. The spin–orbit splitting in the

[54] F. Ajzenberg-Selove and T. Lauritsen, Nucl. Phys. **11**, 1 (1959).

[55] Private communication from the Istituto Superiore di Sanità (Rome) group.[24]

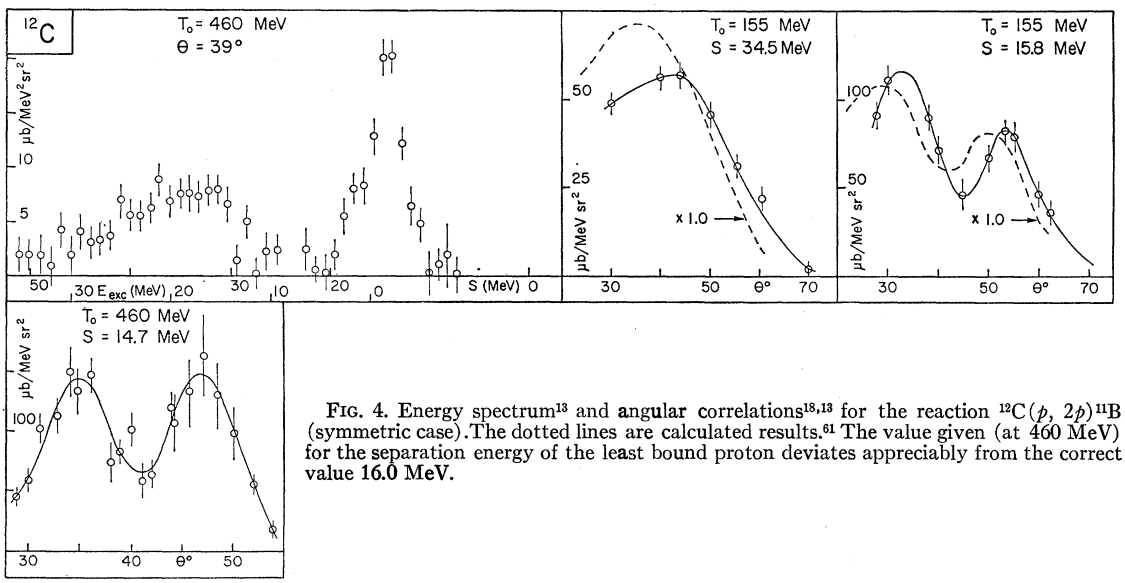

FIG. 4. Energy spectrum[13] and angular correlations[18,13] for the reaction $^{12}C(p, 2p)^{11}B$ (symmetric case). The dotted lines are calculated results.[61] The value given (at 460 MeV) for the separation energy of the least bound proton deviates appreciably from the correct value 16.0 MeV.

$1p$ shell is well resolved; the energies of the two maxima correspond within the experimental accuracy to the $\frac{1}{2}^-$ ground state and to the 6.3 MeV, $\leq\frac{5}{2}^-$ excited state[54] of ^{15}N. The intensity ratio of the two $1p$ shell peaks gives a clear experimental indication of the considerable absorption which already takes place in this light nucleus. Independently of the coupling scheme, one would for this closed shell nucleus expect the $\frac{3}{2}^-$ and $\frac{1}{2}^-$ states of ^{15}N to occur in the ratio 2:1 for all angles. Figure 6 shows that in reality the first excited state results at most angles with about the same probability as the ground state. We shall see below that this difference is naturally explained by the difference in separation energy of the two states.

In each of the investigated $1p$ shell nuclei (see next section) the predicted $1s$ and $1p$ shells have both been observed. For the $2s$–$1d$ shell nuclei the situation is not yet as favorable for the $(p, 2p)$ scattering; besides the upper shell the $1p$ shell has clearly been observed in only one case (^{19}F).

A serious difficulty for the detection of the inner shells is the intensity reduction due to the absorption.

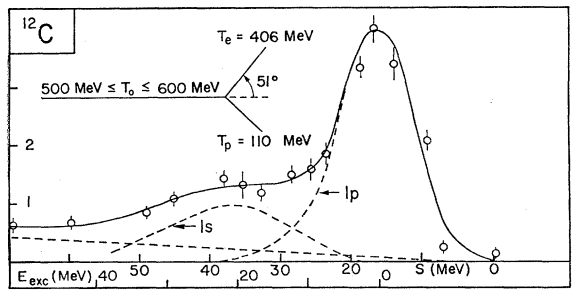

FIG. 5. Energy spectrum[24] for the reaction $^{12}C(e, e'p)^{11}B$ performed in the indicated geometry. The dotted curves give a decomposition in shell contributions and background.

This effect reduces not only the absolute cross sections but also the ratio of the cross sections for inner shells to the ones for upper shells because the last ones predominantly contribute to the nuclear surface. It is therefore perhaps not surprising that in the published investigations by quasi-free electron–proton scattering (on ^{12}C and ^{27}Al) all shells seem to have been observed in both nuclei. As mentioned earlier, another effect which adds to the difficulty of the investigation of inner shells is the increase of the width of a hole state with the number of particles in less bound shells and with the excitation energy of the residual nucleus. This is valid for both the $(p, 2p)$ and the $(e, e'p)$ experiments, and at present it is not known how far the various shells can be followed up.

As examples for the $2s$–$1d$ shell nuclei Figs. 7–10 show the results for ^{19}F, ^{27}Al, and ^{40}Ca. The spectrum of ^{19}F, obtained by the energy sharing experiment, shows three peaks. The distorted momentum distributions in Fig. 7, calculated from the experimental cross section dependence on the energy ratio of the two outgoing particles, agree with the interpretation of an ejection of $2s_{\frac{1}{2}}$, $1p_{\frac{1}{2}}$, and $1p_{\frac{3}{2}}$ protons. The resolution does not seem to be sufficient to observe the energy splittings of each of the two last mentioned groups, expected because of the angular momentum coupling of the hole state with the upper shell. The spin–orbit splitting of the inner $1p$ shell is 8 MeV.

The symmetric $(p, 2p)$ spectrum of ^{27}Al (Fig. 8) shows a maximum, with an only partially resolved structure, leading to an excited state of the residual nucleus ^{26}Mg. The ground state of this nucleus does not seem to be populated. A similar result is found for some other nuclei of the $2s$–$1d$ shell. This may be due to a strong difference in the ground state deformations of the initial and final nucleus but also energy inversions

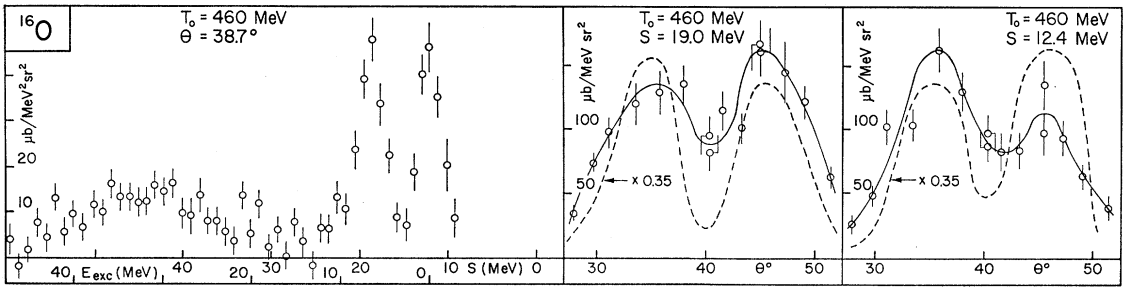

FIG. 6. Energy spectrum and angular correlations[13] for the reaction $^{16}O(p, 2p)^{15}N$ (symmetric case). The dotted lines are calculated results[40] multiplied by the indicated factor.

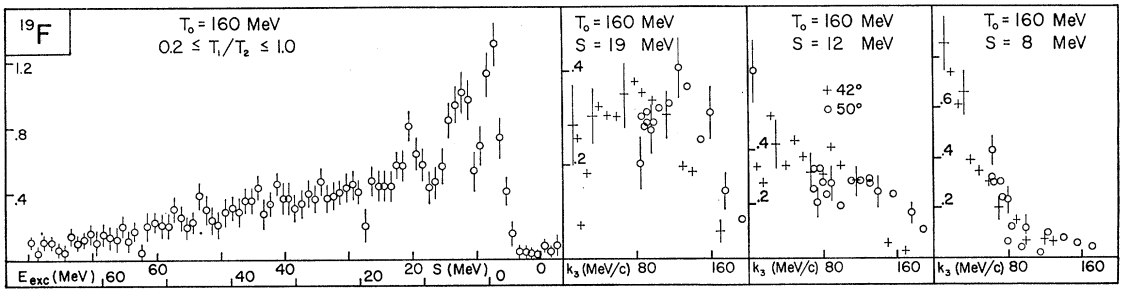

FIG. 7. Energy spectrum and deduced momentum correlations[15] for the reaction $^{19}F(p, 2p)^{18}O$ (energy sharing).

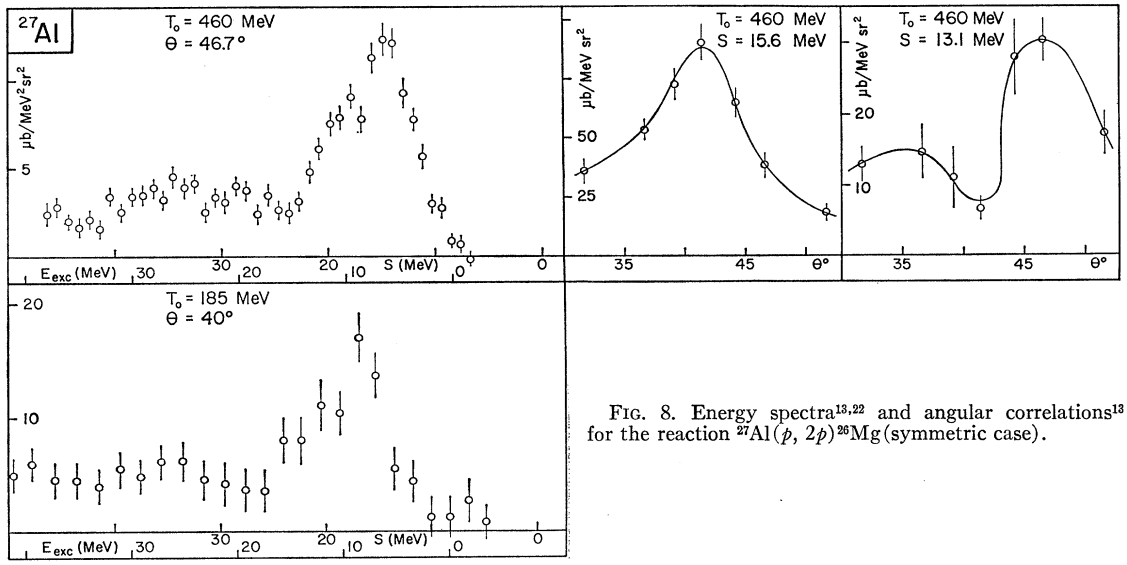

FIG. 8. Energy spectra[13,22] and angular correlations[13] for the reaction $^{27}Al(p, 2p)^{26}Mg$ (symmetric case).

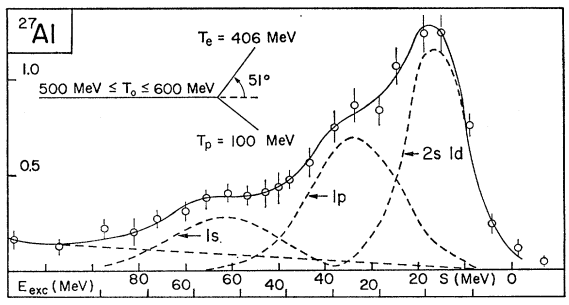

FIG. 9. Energy spectrum[24] for the reaction $^{27}Al(e, e'p)^{26}Mg$ performed in the indicated geometry. The dotted curves give a decomposition in shell contributions and background.

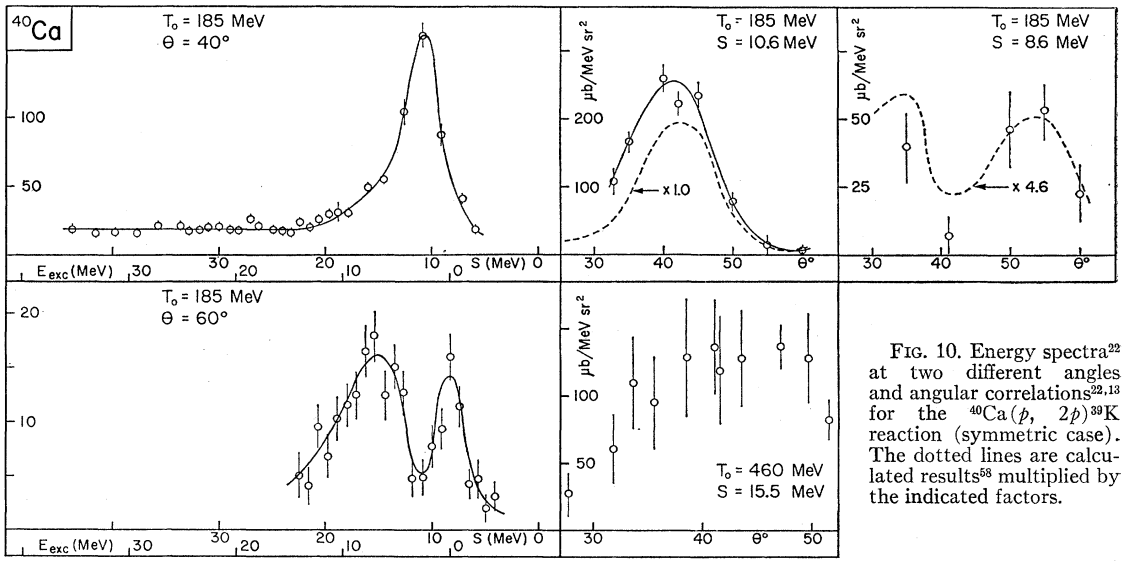

FIG. 10. Energy spectra[22] at two different angles and angular correlations[22,13] for the ^{40}Ca$(p, 2p)^{39}$K reaction (symmetric case). The dotted lines are calculated results[58] multiplied by the indicated factors.

of the $2s$–$1d$ levels may play a role. In Fig. 8 an indication of the $1p$ shell protons may be present between 30 and 40 MeV, but the statistics is not quite sufficient to make this certain.

The spectrum from electron scattering on the same nucleus (Fig. 9) seems not only to show the $1p$ shell protons clearly, but probably also the $1s$ shell maximum; this figure may be compared with the corresponding one for ^{12}C (Fig. 5). The measurement appears to confirm the expected advantage of the quasi-free electron–proton scattering over the proton–proton one for the investigation of inner shells.

The symmetric $(p, 2p)$ spectrum for ^{40}Ca (Fig. 10) shows only upper shell contributions. The angular correlation curves clearly support the shell model assignments of $1d_{\frac{3}{2}}$, $2s_{\frac{1}{2}}$, and $1d_{\frac{5}{2}}$ to the 8.4-, 11.1-, and 14.5-MeV groups, giving 6.1 MeV for the spin–orbit splitting between the $1d_{\frac{3}{2}}$ and $1d_{\frac{5}{2}}$ states.

For nuclei heavier than ^{40}Ca, the measurements are still rather incomplete; these results and the ones for not yet discussed lighter nuclei may be found in the next section.

Figure 11 shows for most measured nuclei the values of the separation energies, the natural widths (corrected for the resolution) of the corresponding hole states and, where available, the orbital angular momentum assignments; for each nucleus we have tried to select the best measurements available. The figure es-

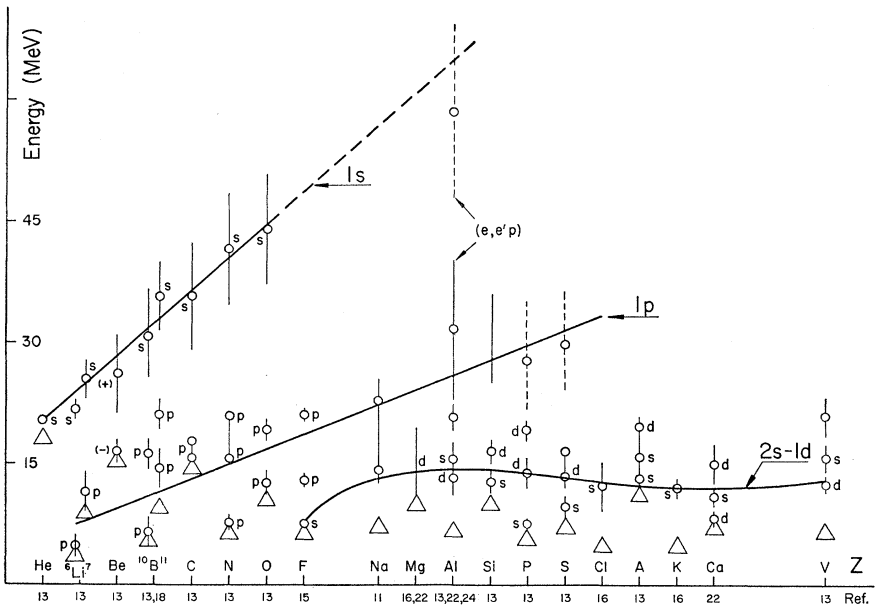

FIG. 11. Separation energies, widths (corrected for resolution) and angular momentum assignments of the hole states from quasi-free scattering as functions of the atomic number. The angular momentum assignments are given if unique on the basis of a correlation distribution assuming the validity of the shell model. The position of a clear maximum is indicated by a circle; uncertain levels are dotted. The triangles indicate the separation energy of the least bound proton; references are given under the abscissa. The full lines, meant as guides for the eye, crudely follow the shells.

TABLE II. Distorted wave calculations for quasi-free scattering with incoming energies larger than 100 MeV.

Authors	Reaction	Energies	Nuclei	Remarks
Berggren (Ref. 66)	$(p, 2p)$	460 MeV	^{4}He, ^{6}Li, 7Li, ^{8}Be, ^{12}C, ^{14}N, ^{16}O	semiclassical calculation
Berggren and Jacob (Ref. 40)	$(p, 2p)$	170 MeV	^{6}Li, ^{7}Li, ^{9}Be, ^{10}B, ^{11}B, ^{12}C, ^{16}O (also 450 MeV) ^{6}Li	semiclassical calculation
Jackson and Berggren (Ref. 48)	$(p, 2p)$	185 MeV	^{6}Li	phase shift analysis
Jacob and Maris (Ref. 23)	$(e, e'p)$	300–1000 MeV	^{12}C, ^{40}Ca, and interpolation graph for nuclei with $4 \leqslant A \leqslant 60$	semiclassical calculation
Johansson and Sakamoto (Ref. 57)	$(p, 2p)$	180 MeV	^{6}Li, ^{7}Li	semiclassical calculation
Johansson and Tibell (Ref. 58)	$(p, 2p)$	180 MeV	^{27}Al, ^{31}P, ^{40}Ca	semiclassical calculation
Lim and McCarthy (Ref. 47)	$(p, 2p)$	155 MeV	^{6}Li, ^{7}Li, ^{10}B, ^{11}B, ^{12}C	phase shift analysis
Maris (Ref. 35)	$(p, 2p)$	180 and 400 MeV	^{7}Li	semiclassical calculation
Riley, Pugh, and Gooding (Ref. 52)	$(p, 2p)$	153 MeV	^{12}C	asymmetric; semiclassical calculation
Rosenblum (Ref. 59)	$(p, 2p)$	100, 180 and 400 MeV	^{7}Li	semiclassical calculation
Sakamoto (Refs. 60, 61)	$(p, 2p)$	185 and 155 MeV	^{6}Li, ^{12}C	semiclassical calculation
Strnad (Ref. 62)	$(p, 2p)$	155 MeV	^{12}C	semiclassical calculation
Takemiya (Ref. 63)	$(p, 2p)$	155 MeV	^{6}Li, ^{7}Li	distortion calculated from double scattering

sentially contains the only direct experimental information which is known at the time of writing (June 1965) on the separation energies and widths of inner shell states in light nuclei. The full lines are drawn to guide the eye along levels belonging to the same shell. Towards increasing values of Z there is a clear tendency of the curves to diverge. For separation energies of single-particle states generated by a static potential which only increases in size for increasing values of A, one would expect the curves to converge. A comparison of these results with expectations from nuclear theory is however beyond the scope of the present review; for calculations of inner shell energies see Ref. 56.

Figure 12 shows the natural width of the measured $1s$ states as a function of A. Evidently it is a strongly increasing function. This is understandable from the fact that in the shell model the mechanism which in lowest order causes the decay of these states is the one in which the hole is filled by an interaction (collision) between a proton of the $1p$ shell with another nucleon in the same shell. For the $1p$ shell nuclei one would therefore crudely expect the width of the $1s$ hole state to be directly proportional to the number of proton–nucleon pairs in the $1p$ shell and inversely proportional to the nuclear volume.[34] The dotted line shows this dependence, normalized at ^{14}N.

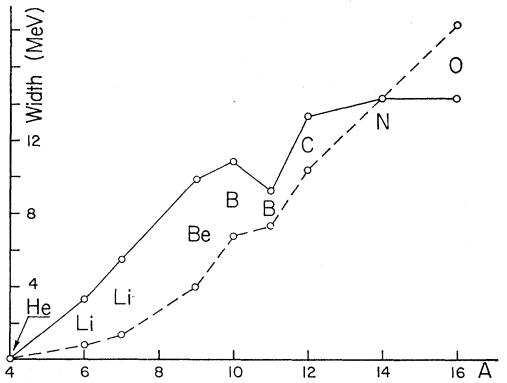

FIG. 12. Experimental (full line) and estimated (dotted line) widths of the $1s$ hole states for the $1p$ shell nuclei.

[56] W. E. Frahn and R. H. Lemmer, Nuovo Cimento **6**, 1221 (1957); K. A. Brueckner, A. M. Lockett, and M. Rotenberg, Phys. Rev. **121**, 255 (1961); D. M. Brink and N. Sherman, Phys. Rev. Letters **11**, 393 (1965); H. S. Köhler, Phys. Rev. **138**, B831 (1965).
[57] A. Johansson and Y. Sakamoto, Nucl. Phys. **42**, 625 (1963).
[58] A. Johansson and G. Tibell, quoted in Ref. 22.
[59] W. M. Rosenblum, master thesis, Florida State University (1960).
[60] Y. Sakamoto, Phys. Letters **1**, 256 (1962); Y. Sakamoto, Nuovo Cimento **26**, 461 (1962).
[61] Y. Sakamoto, Progr. Theoret. Phys. (Kyoto) **28**, 803 (1962).
[62] J. Strnad, Glasnik Mat.-Fiz. Astron. **17**, 89 (1962).
[63] T. Takemiya, Progr. Theoret. Phys. (Kyoto) **30**, 191 (1963).

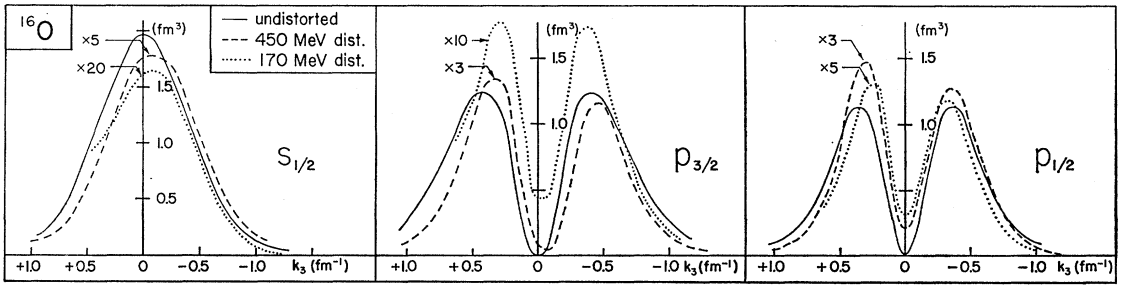

FIG. 13. Calculated undistorted and distorted (multiplied by the indicated factors) momentum distributions,[40] for the reaction $^{16}O(p, 2p)^{15}N$ (symmetric case) at 450 and 170 MeV.

B. Calculated Results

The determination of the cross section Eq. (3.33) amounts to a computation of the distorted momentum distribution

$$\sum_{m_{A-1},m_A} \sum_{n} | g'^{(n)}_{m_{A-1},m_A}(\mathbf{k}_1+\mathbf{k}_2-\mathbf{k}_0) |^2$$

defined in Eq. (3.27). Up to now this function has been determined in two quite different approximations, namely, either by neglecting the distortion or by assuming a j–j coupled extreme single-particle model.

In the first mentioned type of work,[30,31] the one-particle fractional parentages of the states excited in the residual nucleus with respect to the ground state of the initial nucleus are determined using some model. The results predict which final nuclear states are expected to occur with an appreciable probability. Neglect of the distortion is, however, serious. It affects the cross section for different states by different angle-dependent factors, and therefore, it is not possible to derive reliable values for the fractional parentage coefficients from the experimental results without taking distortion into account. The dependence of the distortion on the properties of the overlap integral are clearly shown below for ^{16}O (see Fig. 13).

A considerable amount of work (see Table II) has been done simply using j–j coupled single-particle wave functions but taking the distortion of the plane proton waves into account. For closed shells this seems to be the natural approach; but also in some other cases the results of this type of calculation may be compared with experiments after summing the contributions from certain final states. In these cases the distortion is again not quite correctly taken into account. As this work is of interest for the understanding of the reaction and may directly be compared with measurements, we now discuss this type of calculation in more detail and give some results. Very recent calculations by Berggren[64] could not be included anymore.

As we have seen, an angular correlation measurement is helpful for the determination of the quantum numbers of a peak in the energy spectrum; however, more detailed information on the wave function in momentum space, though in principle contained in an angular correlation curve, is in practice not yet obtainable. Mainly due to the uncertainty in the distortion of the plane proton waves, comparisons of the results of calculations with measurements are still in a somewhat exploratory stage. The analysis however shows that the shapes and the orders of magnitude of the correlation distributions are in agreement with the basic model for this reaction.

The most extensive calculations have been performed for ^6Li. The results (dotted lines) in Fig. 3, taken from Ref. 57, show that the agreement with the experimental data is promising though the filling in of the minimum for the $1p$ correlation is insufficient.[65] In this calculation numerical wave functions, obtained from a truncated harmonic oscillator potential with an exponential tail, have been used and the distortion has been taken into account in the semiclassical way using square well potentials. In Ref. 57 it is also shown how seemingly small variations in the shape of the wave functions may have a relatively large infiuence on the cross section.

The results[61] for ^{12}C in Fig. 4 are in a surprising agreement[65] with the experimental ones, considering the simplicity of the calculations, in which infinite harmonic oscillator wave functions and purely imaginary square well potentials in a semiclassical approximation for the distortions have been used.

For ^{16}O the dotted curves shown in Fig. 6 have been calculated[40] with exponential wave functions and with Gaussian complex potentials in a semiclassical approximation for the distortion. The calculated results are about three times larger than the experimental ones, but the ratio of the magnitudes of the calculated $1p_{\frac{1}{2}}$ and $1p_{\frac{3}{2}}$ distributions is approximately correct. The deviation of the experimental result from the expected ratio of two can be traced to the effect of the separation energy on the absorption and on the momentum distribution, which has already been discussed for the case of ^6Li in the preceding subsection. The asymmetries in the calculated and the experimental curves are just opposite, a result for which we do not have a simple explanation.

[64] H. Tyrén, S. Kullander, O. Sundberg, R. Ramachandran, P. I. Isaacson, and T. Berggren, preprint (to be published).

[65] Recent measurements[16] on ^{12}C indicate, however, that the depth of the measured minimum is very sensitively dependent on the angular resolution.

The calculated curves[58] shown in Fig. 10 for ^{40}Ca have been obtained in a similar way as the ones for ^{6}Li. Except for the magnitude of the $1d_{\frac{3}{2}}$ state the agreement is good, showing that even for a relatively heavy nucleus the simple model used still works rather well.

In order to compare the influence of absorption at different energies, we give in Fig. 13 the undistorted and the distorted momentum distributions for ^{16}O at 170 and 450 MeV calculated in the same way as the previous results for this nucleus; the $1s$ wave function has been taken of the harmonic oscillator type. One sees that the influence of distortion is larger for smaller bombarding energies and for states with higher binding energies; this result was anticipated in Sec. II and seems to imply an advantage of experiments at higher energies.

Figure 14 shows the calculated results of the distorted and undistorted momentum distributions for an $(e, e'p)$ reaction on ^{40}Ca. The wave functions have been obtained from a harmonic oscillator potential, and the plane proton wave has been distorted by an imaginary Gaussian potential in the semiclassical approximation; the electron wave functions have been taken as plane waves. One clearly sees that the expected effect of multiple collisions is not very important; the distorted distributions have nearly the shape of the undistorted ones and the reduction of the size of the cross section is orders of magnitude smaller than in the case of $(p, 2p)$ scattering, in agreement with the qualitative discussion of Sec. II.

V. RESULTS FOR OTHER NUCLEI

This section is meant for readers who are interested in detailed data for nuclei other than those which have been considered as examples in the preceding section. As in the other sections, we do not go into the implications which the experimental results may have for the detailed structure of the individual nuclei.

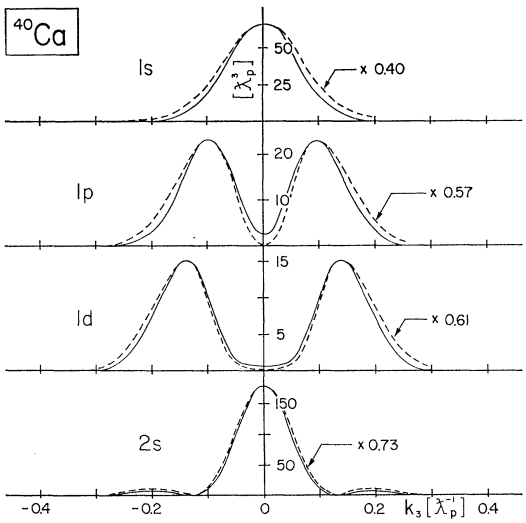

FIG. 14. Calculated undistorted (multiplied by the indicated factors) and distorted momentum distributions,[23] for the reaction ^{40}Ca$(e, e'p)^{39}$K; incident electron energy between 300 and 1000 MeV, proton energy between 150 and 400 MeV; the unit of length is the reduced proton Compton wavelength.

Typical measurements for the $1p$ shell nuclei are shown in Fig. 15. In all nuclei one sees the $1s$ and $1p$ maxima in the energy spectrum; these assignments are supported by the angular correlations.

In some cases the upper shell peaks clearly show a structure, which should be understandable from a fractional parentage analysis[9]; as remarked earlier, calculations neglecting distortion[30,31] should however be considered with caution. The spin–orbit splitting of the $1p$ shell and the increase of the width of the $1s$ shell with A are clearly seen in the figure. Probably in all cases (except ^{11}B) the residual nucleus remains rather frequently in its ground state, which shows that this state has a considerable overlap with the ground state of the initial nucleus.

In general the separation energies (see Fig. 11 of the preceding section) vary smoothly from nucleus to nucleus, except in the case of ^{9}Be. This exception is not quite unexpected as this nucleus is generally assumed in the shell model to be strongly deformed and is probably more naturally described by a cluster model.[44] The angular correlations indicate that the parity assignments of the two energy maxima in the ^{9}Be spectrum are still the ones suggested by the extreme single-particle model.

The effect of the extra neutron in ^{11}B as compared to ^{10}B is an increase of the separation energy by about 3 MeV and of the absorption by a factor of about 1.5.

The calculated angular correlation curves (dotted in the figures) show a semiquantitative agreement with the measuremenrs[66]; in general the minimum in the $1p$ distribution is not sufficiently filled (see, however, footnote 65). In contradistinction to the earlier case of ^{16}O, the asymmetry in this distribution around the "free" scattering angle is in general reasonably well reproduced.

Figure 16 shows a selection of energy spectra and angular correlations for several of the $2s$–$1d$ shell nuclei. The information available in this case is less extensive than for the $1p$ shell nuclei. The transition to the ground state of the residual nucleus is absent in several spectra as already discussed in the last section. (Note also the discrepancy in the energy scales of the two ^{24}Mg spectra.) In a few nuclei indications of the $1p$ shell are visible in the energy spectrum.

If momentum correlations of the peaks in an energy spectrum are measured, a $2s$ level is easily recognizable by its sharp maximum at the "free" scattering momenta. The minimum at this point in the correlation curves for $1d$ protons (positive parity!) may be completely filled, but the curves are still much flatter than the $2s$ ones.

The information available for nuclei heavier than ^{40}Ca is still very incomplete. Because of the larger absorption

[66] The absolute cross sections of some $1p$ shell nuclei determined by the Orsay[18,19] (155 MeV) and Uppsala[22] (185 MeV) groups differ by a factor of about three.

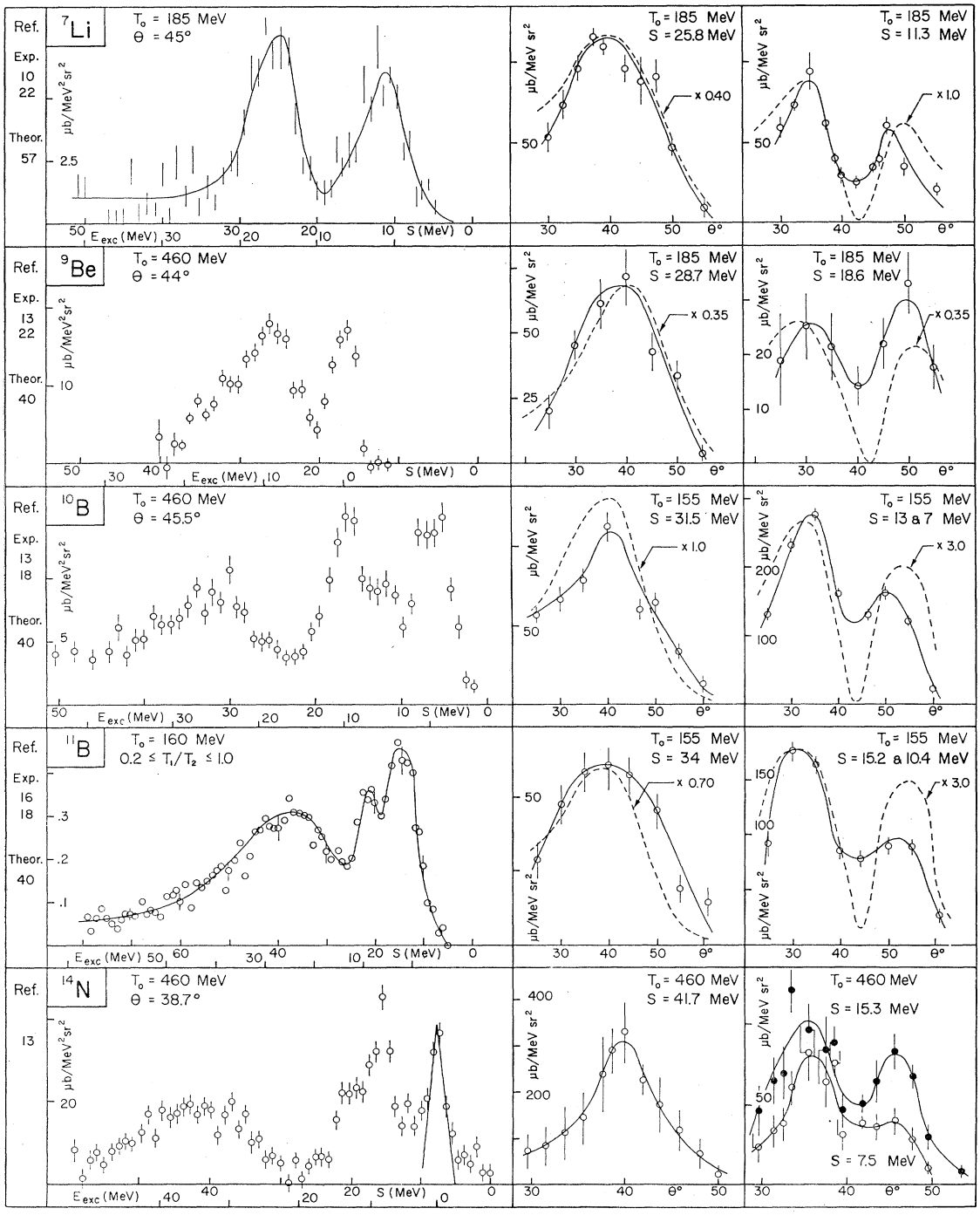

FIG. 15. Energy spectra and angular correlations for some $1p$ shell nuclei from $(p, 2p)$ experiments. Dotted lines represent calculated results multiplied by the indicated factors.

and smaller energy differences between the shells the experimental difficulties tend to increase with increasing atomic number. The most extensive measurements have been reported in Ref. 20. Figure 17 shows the examples of ^{51}V and ^{52}Cr. As in previous cases a $2s$ state is easily recognizable by its large contribution at zero momentum transfer, but not much can be said before more detailed results are available.

VI. CONCLUDING REMARKS

From the comparison of the expectations based on the model described in the preceding sections with the experimental results, it seems fair to conclude that our interpretation of the quasi-free reaction is essentially correct. The general structure of the energy spectra and the shapes of the correlation curves are under-

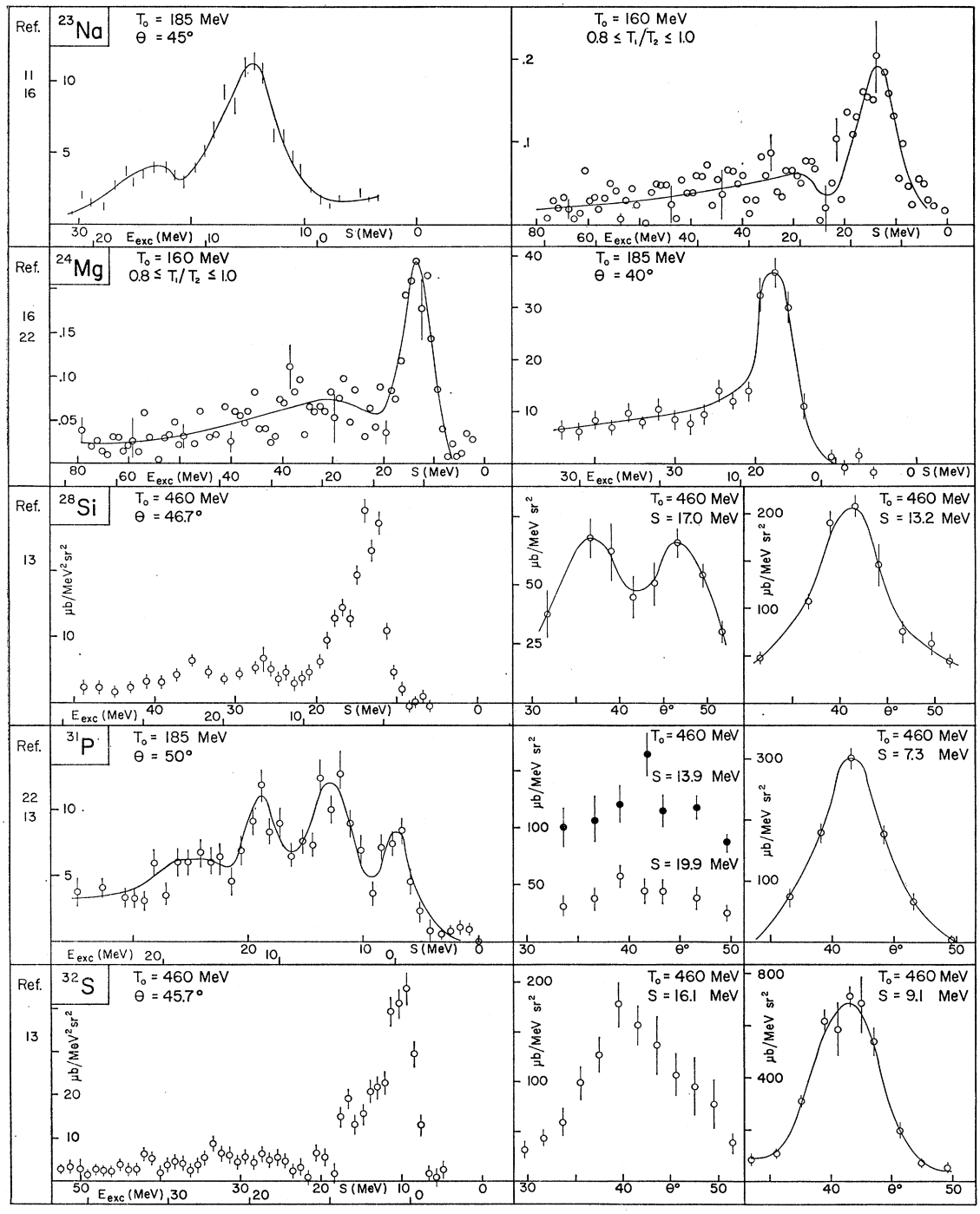

FIG. 16. Energy spectrum and angular correlations for some $2s$–$1d$ shell nuclei from $(p, 2p)$ experiments.

stood; also, the orders of magnitude of the experimental cross sections agree with the calculated ones. At present the graph of the separation energies and hole state widths for the various shells (Fig. 11) seems to be the most interesting information supplied by the reaction under discussion.

Though one might hope ultimately to obtain detailed information on the low momentum region of the momentum distributions of the various shells, at the present time we seem to be still distant from this aim. In fact, the agreement between the calculated and measured correlation cross sections is only a very crude one, both with respect to absolute magnitudes and to relative ones for different angles, energies and nuclei. This is not surprising if one observes how sensitively the calculated cross sections depend on the nuclear

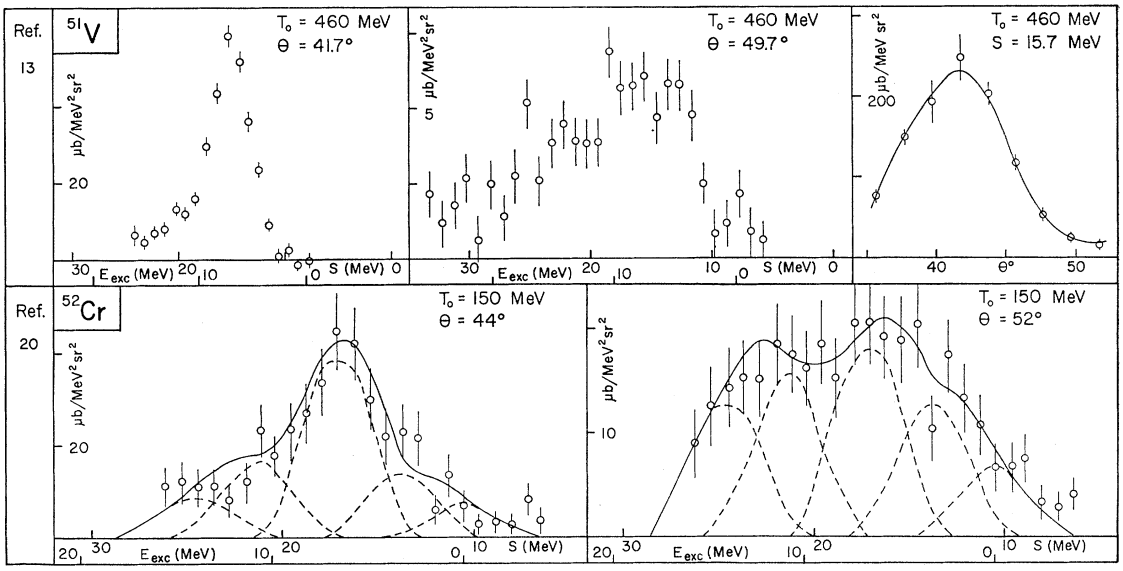

FIG. 17. Energy spectra and angular correlations for two nuclei of the $2p$–$1f$ shell from $(p, 2p)$ experiments. The dotted lines are tentative decompositions of the spectra performed by the authors of the original publication.

wave function and the distorted plane waves which are used. In particular, the relation of the shape and size of the selected shell model potential to those of the imaginary parts of the optical potentials which distort the plane waves should be quite essential and has up to now only crudely been taken into account in the performed calculations.

How details in the wave function may influence the experimental result has been most directly seen in the deviation from the constant value two of the ratio of the cross sections for the $1p_{\frac{3}{2}}$ and $1p_{\frac{1}{2}}$ protons in ^{16}O. It is encouraging that calculations approximately reproduce this deviation, showing that it is mainly caused by the difference in the exponential tails of the single-particle wave functions due to the differing separation energies.

The expected decrease of the absorption, when varying the bombarding energy from 150 to 450 MeV, has experimentally not yet been clearly confirmed. Where the absolute cross sections are measured at both energies no calculations exist and vice-versa.

Theoretically the electron–proton quasi-free scattering promises to have many advantages over the proton–proton one because the nuclear transparency for the former process is expected to be about equal to the third root of the transparency for the latter. This would seem to offer an opportunity to observe more inner shells, and the distortion of the momentum distributions is expected to be much smaller.

Experimentally the optimum electron beam for this type of measurement would be an external one with a well defined energy between 500 and 1000 MeV, a high intensity and a high duty cycle. In planning future electron accelerators in the considered energy range these conditions could be of interest.

The $(e, e'p)$ experiment is difficult because of the smallness of the electromagnetic cross section, and the strong energy–momentum dependence of this cross section possibly requires a special geometry to obtain reliable correlation curves. The first measurements performed on complex nuclei seem, however, to give reason for optimism.

ACKNOWLEDGMENTS

We are indebted to the experimental groups of Chicago, Rome, Harvard, Orsay, and Uppsala for keeping us continuously informed on their work and for allowing us to include several unpublished results. We thank our colleagues Darcy Dillenburg, John D. Rogers, and Marcus Zwanziger for valuable comments and for help in the preparation of the manuscript. One of us (T.M.) thanks the members of this Institute for their warm hospitality; his stay at this University has been made possible through the Professorship Program of the Pan American Union.

This work has been supported by the Pan American Union, by the U. S. Army Research Office, and by the Conselho Nacional de Pesquisas, Brazil.